2

NASA TECHNICAL MEMORANDUM

NASA TM X-62,203

NASA TM X-62,203

PITCH ATTITUDE, FLIGHT PATH, AND AIRSPEED CONTROL DURING APPROACH AND LANDING OF A POWERED LIFT STOL AIRCRAFT

James A. Franklin and Robert C. Innis

Ames Research Center
Moffett Field, California 94035

December 1972

PITCH ATTITUDE, FLIGHT PATH, AND AIRSPEED CONTROL DURING APPROACH AND LANDING OF A POWERED LIFT STOL AIRCRAFT

James A. Franklin and Robert C. Innis

Ames Research Center
Moffett Field, California, 94035

SUMMARY

Analytical investigations and piloted moving base simulator evaluations were conducted for manual control of pitch attitude, flight path, and airspeed for the approach and landing of a powered lift jet STOL aircraft. Flight path and speed response characteristics were described analytically and were evaluated for the simulation experiments which were carried out on a large motion simulator (FSAA) at Ames Research Center. The response characteristics were selected and evaluated for a specified path and speed control technique. These characteristics were (1) the initial pitch response and steady pitch rate sensitivity for control of attitude with a pitch rate command/attitude hold system, (2) the initial flight path response, flight path overshoot, and flight path-airspeed coupling in response to a change in thrust, and (3) the sensitivity of airspeed to pitch attitude changes. Results are presented in the form of pilot opinion ratings and commentary, substantiated where appropriate by response time histories and aircraft states at the point of touchdown.

NOTATION

A_{uT}	Gain of the thrust to speed transfer function, ft/sec/lb
$A_{u\theta}$	Gain of the attitude to speed transfer function, ft/sec/rad
$A_{\gamma T}$	Gain of the thrust to flight path transfer function, rad/lb
$A_{\gamma\theta}$	Gain of the attitude to flight path transfer function, rad/rad
a_z	Normal acceleration, g's

c_j	Thrust coefficient for cold blowing air, $T_{cold}/\bar{q}S_w$
db	Decibels
$d\gamma/dV$	Change of flight path with airspeed for constant thrust, deg/kt
F_c	Pilot's control column force, lbs
GW	Gross weight, lbs
g	Acceleration due to gravity, ft/sec^2
H_{δ_e}	Dimensional elevator hinge moment derivative due to elevator deflection, $1/I_e\ (\partial H_e/\partial \delta_e)$, $rad/sec^2/rad$
$H_{\dot{\delta}_e}$	Dimensional elevator hinge moment derivative due to elevator deflection rate, $1/I_e\ (\partial H_e/\partial \dot{\delta}_e)$, 1/sec
h	Altitude, ft
$\dot{h}$	Vertical velocity, ft/sec or ft/min
IFR	Instrument flight rules
ILS	Instrument landing system
I_e	Elevator moment of inertia, $slug\text{-}ft^2$
I_x	Roll moment of inertia, $slug\text{-}ft^2$
I_y	Pitch moment of inertia, $slug\text{-}ft^2$
I_z	Yaw moment of inertia, $slug\text{-}ft^2$
I_{xz}	Cross-product of inertia, $slug\text{-}ft^2$
j	Complex number, $(-1)^{1/2}$
K_I	Gain for pitch rate command integrator, deg/sec/in
K_q	Pitch rate feedback gain to elevator, deg/deg/sec

K_u	Airspeed feedback gain to nozzle, deg/kt
K_α	Angle of attack feedback gain to nozzle, deg/deg
K_δ	Column position feedforward gain, deg/in
K_θ	Pitch attitude feedback gain to elevator, deg/deg
M	Pitching moment, ft-lbs
m	Aircraft mass, slugs
M_q	Pitch rate damping, $1/I_y$ $(\partial M/\partial q)$,1/sec
M_u	Pitch acceleration derivative due to forward speed, $1/I_y$ $(\partial M/\partial u)$,rad/sec^2 per ft/sec
M_α	Longitudinal static angle of attack stability, $1/I_y$ $(\partial M/\partial \alpha)$,rad/sec^2/rad
$M_{\dot{\alpha}}$	Pitch acceleration derivative due to rate of change of angle of attack, $1/I_y$ $(\partial M/\partial \dot{\alpha})$,1/sec
M_{δ_e}	Elevator control effectiveness, $1/I_y$ $(\partial M/\partial \delta_e)$, rad/sec^2/rad
M_{δ_T}	Pitch acceleration derivative due to thrust, $1/I_y$ $(\partial M/\partial \delta_T)$,rad/sec^2/lb
M_{δ_ν}	Pitch acceleration derivative due to nozzle deflection, $1/I_y$ $(\partial M/\partial \delta_\nu)$,rad/sec^2/rad
N_i^r	Numerator of the transfer function relating the response r to an input i
$N_{\delta_e \delta_T}^{\theta\gamma}$	Coupling numerator for flight path response to thrust with attitude to elevator loop closed
$N_{\delta_T \delta_e}^{u\theta}$	Coupling numerator for airspeed response to thrust with attitude to elevator loop closed
q, q_B	Body axis pitch rate, deg/sec
$\bar{q}$	Dynamic pressure, lbs/ft^2
S_W	Wing area, ft^2

s	Laplace operator, $\sigma \pm j\omega$
t	Time, sec
T_{hot}	Component of thrust due to hot jet exhaust, lbs
T_{cold}	Thrust of cold blowing air from augmentor flap, lbs
T_{L_θ}	Lead time constant for the $\theta \rightarrow \delta_e$ loop
$1/T_{sp_1}$, $1/T_{sp_2}$	Real roots of the longitudinal characteristic equation normally associated with the short period mode
$1/T'_{sp_1}$, $1/T'_{sp_2}$	Real roots of the longitudinal characteristic equation (with the $\theta \rightarrow \delta_e$ loop closed) normally associated with the short period mode
$1/T_{u_T}$	Low frequency root of the numerator of the thrust to airspeed transfer function with the attitude to elevator loop closed
$1/T_{u_\theta}$	Low frequency root of the numerator of the attitude to airspeed transfer function
$1/T_{\gamma_T}$	Low frequency root of the numerator of the thrust to flight path transfer function with the attitude to elevator loop closed
$1/T_{\gamma_\theta}$	Low frequency root of the numerator of the attitude to flight path transfer function (frequently identified in the literature as $1/T_{h_1}$ - the low frequency numerator factor of the elevator to altitude transfer function)
T_δ	Pitch rate command system time constant
$1/T_{\theta_1}$, $1/T_{\theta_2}$	Real roots of the numerator of the elevator to attitude transfer function
$1/T'_{\theta_1}$, $1/T'_{\theta_2}$	Low frequency real roots of the longitudinal characteristic equation (with the $\theta \rightarrow \delta_e$ loop closed) normally associated with the phugoid mode
u	Perturbation airspeed, knots or ft/sec

u_c	Commanded airspeed perturbation, knots or ft/sec
V_o	True airspeed, knots or ft/sec
VFR	Visual flight rules
X	Longitudinal force, lbs
x_{cg}	Center of gravity location, % mean aerodynamic chord
X_q	Longitudinal acceleration derivative due to pitch rate, 1/m ($\partial X/\partial q$),ft/sec
X_u	Longitudinal acceleration derivative due to forward speed, 1/m ($\partial X/\partial u$),1/sec
X_α	Longitudinal acceleration derivative due to angle of attack, 1/m ($\partial X/\partial \alpha$),ft/sec^2/rad
$X_{\dot{\alpha}}$	Longitudinal acceleration derivative due to angle of attack rate, 1/m ($\partial X/\partial \dot{\alpha}$),ft/sec
X_{δ_e}	Elevator drag derivative, 1/m ($\partial X/\partial \delta_e$), ft/sec^2/rad
X_{δ_T}	Longitudinal acceleration derivative due to thrust, 1/m ($\partial X/\partial \delta_T$),ft/sec^2/lb
X_{δ_ν}	Longitudinal acceleration derivative due to nozzle deflection, 1/m ($\partial X/\partial \delta_\nu$),ft/sec^2/rad
Y_u	Transfer function for speed control with attitude
Y_γ	Transfer function for flight path control with thrust
Y_θ	Transfer function for attitude control with elevator
Z	Vertical force, lbs
Z_q	Vertical acceleration derivative due to pitch rate, 1/m ($\partial Z/\partial q$),ft/sec
Z_u	Vertical acceleration derivative due to forward speed, 1/m ($\partial Z/\partial u$),1/sec

Z_α	Vertical acceleration derivative due to angle of attack, 1/m $(\partial Z/\partial \alpha)$, ft/sec^2/rad
$Z_{\dot{\alpha}}$	Vertical acceleration derivative due to angle of attack rate, 1/m $(\partial Z/\partial \dot{\alpha})$, ft/sec
Z_{δ_e}	Elevator lift derivative, 1/m $(\partial Z/\partial \delta_e)$, ft/sec^2/rad
Z_{δ_T}	Vertical acceleration derivative due to thrust, 1/m $(\partial Z/\partial \delta_T)$, ft/sec^2/lb
Z_{δ_ν}	Vertical acceleration derivative due to nozzle deflection, 1/m $(\partial Z/\partial \delta_\nu)$, ft/sec^2/rad
α	Angle of attack, deg or rad
γ	Flight path angle, deg or rad
γ_c	Commanded flight path angle, deg or rad
γ_{ss}	Steady state flight path angle, deg or rad
Δ	Characteristic matrix for longitudinal equations of motion; incremental value
$\left(\frac{\Delta u_{ss}}{\Delta \gamma_{ss}}\right)_{\Delta T}$	Ratio of change of steady state airspeed to flight path due to a change in thrust (constant pitch attitude), knots/deg
$\frac{\Delta u_{ss}}{\Delta \theta}$	Change in steady state airspeed per unit change in pitch attitude (constant thrust), knots/deg
$\Delta\gamma_{max}$	Maximum flight path change following a change in thrust, deg
$\left(\frac{\Delta\gamma_{max}}{\Delta\gamma_{ss}}\right)_{\Delta T}$	Ratio of maximum to steady state change of flight path due to a change in thrust (constant pitch attitude)
δ_c	Control column deflection, in
δ_e	Elevator deflection, deg
δ_{e_c}	Commanded elevator deflection, deg
δ_f	Flap deflection, deg
δ_T	Throttle deflection, deg; change in thrust, lbs

δ_ν	Nozzle deflection, deg
ζ_p, ω_p	Damping ratio and natural frequency of the phugoid mode
ζ'_p, ω'_p	Damping ratio and natural frequency of the phugoid mode (with the $\theta \rightarrow \delta_e$ loop closed)
ζ_{sp}, ω_{sp}	Damping ratio and natural frequency of the short period mode
$\zeta'_{sp}, \omega'_{sp}$	Damping ratio and natural frequency of the short period mode (with the $\theta \rightarrow \delta_e$ loop closed)
$\zeta_\theta, \omega_\theta$	Damping ratio and natural frequency of the numerator roots of the elevator to attitude transfer function
σ	Real part of a complex root
ω	Frequency, rad/sec
τ_γ	Time constant for initial flight path response to thrust, sec
θ	Pitch attitude, deg
θ_c	Commanded pitch attitude, deg
θ_ε	Pitch attitude error, deg
$\dot{\theta}_{max}$	Maximum pitch rate response to elevator, deg/sec
$\dot{\theta}_{ss}$	Steady state pitch rate response to elevator, deg/sec
θ_T	Effective thrust inclination, deg
$\dot{(\ )}$	Derivative with respect to time, d( )/dt
$\lvert(\ )\rvert$	Absolute value of ( )
$\angle(\ )$	Phase angle of ( )
$\doteq$	Approximately equal to

INTRODUCTION

Manual control of a transport aircraft which is capable of operation at speeds within the STOL flight regime, and which utilizes significant amounts of power to augment its basic aerodynamics is generally more difficult than control of conventional aircraft operating at higher speeds. In particular, longitudinal control is adversely affected by the low speed, high wing loading, and high inertias typical of this category of aircraft.

This report presents results of an analytical and experimental investigation of some of the longitudinal control problems of concern. The purpose of the analytical study was to describe the features which characterize pitch attitude, flight path, and speed response to the pilot, and to identify the contribution to these response characteristics of aircraft configuration and flight condition. The results of the analysis were used to guide an experimental investigation conducted on a large motion aircraft simulator. Pilot evaluations were obtained in this investigation to define the relative importance of the significant response characteristics to manual control of the STOL approach and landing.

ANALYTICAL INVESTIGATION

Pitch Attitude Control

Precise control of pitch attitude is essential for control of flight path and airspeed during the landing approach. Effort demanded of the pilot to overcome deficiencies in attitude control associated with sluggish attitude response and strong phugoid excitation creates a workload which can seriously detract from his performance of the overall STOL landing. Consequently, stability and command augmentation is frequently incorporated in the longitudinal control system of these vehicles. These augmentation systems typically take the form of attitude command or rate command/attitude hold systems. The current study concentrated on evaluation of a pitch rate command/pitch attitude hold system.

The system is shown conceptually in the block diagram of Figure 1. The system can be tailored to provide pitch rate proportional to the pilot's command input with pitch attitude hold when the control is neutralized. This system improves precision of attitude control and reduces the pilot's workload by effectively trimming the airplane at the desired attitude. Control sensitivity can be tailored to the pilot's preference.

The significant characteristics of the rate command system's response can best be appreciated by considering the separate contributions of the attitude and rate feedbacks which provide pitch damping and stabilization, and the command inputs proportional to control displacement and its time integral. Closing the pitch rate and attitude loops alters the airplane's short period and phugoid roots and the pitch attitude transfer function as shown in Figure 2. Both short period and phugoid mode damping are improved considerably resulting in the virtual suppression of the phugoid mode. The closed loop attitude transfer function effectively takes on the character of a second order system with high damping due to the near cancellation of the closed loop roots associated with the phugoid and the attitude numerator roots at ω_θ, i.e.,

$$\frac{\theta}{\theta_c} = \frac{N^{\theta}_{\delta e}}{\Delta + \left(K_q s + K_\theta\right) N^{\theta}_{\delta e}} = \frac{M_{\delta e}\left(s^2 + 2\zeta_\theta \omega_\theta s + \omega_\theta^2\right)}{\left(s^2 + 2\zeta\omega'_p s + \omega'^2_p\right)\left(s + 1/T'_{sp_1}\right)\left(s + 1/T'_{sp_2}\right)} \quad (1)$$

*

or by approximate cancellation of terms

$$\frac{\theta}{\theta_c} \doteq \frac{M_{\delta e}}{\left(s + 1/T'_{sp_1}\right)\left(s + 1/T'_{sp_2}\right)} \quad (2)$$

This result is readily observed in the Bode plot of Figure 3a. Adding the rate command elements to the forward loop modifies the transfer function of equation (2) to the form

$$\frac{\theta}{\delta_c} \doteq K_\delta M_{\delta e}\left[\frac{\left(T_\delta s + 1\right)}{s\left(s + 1/T'_{sp_1}\right)\left(s + 1/T'_{sp_2}\right)}\right] \quad (3)$$

which is illustrated in Figure 3b. The form of this attitude transfer function is equivalent to the idealized short period approximation to the open loop attitude response to elevator, $\theta/\delta e$. In the closed loop equation (3), the numerator factor $(s + 1/T_\delta)$ is equivalent to the $(s + 1/T_{\theta_2})$ factor of the traditional θ/δ_e transfer function, while the closed loop short period mode bears obvious resemblance to its open loop counterpart. Such similarity leads to the inference that characteristics of the open loop attitude response to elevator which are important for manual control will be of similar importance in the equivalent closed loop case; further, that characteristics of the open loop response given good pilot ratings would be similarly rated for the rate command system.

---

*Strictly speaking, the attitude numerator

$$N^{\theta}_{\delta_e} = M_{\delta_e}\left[s^2 + \left(X_u + \frac{Z_\alpha}{V_o}\right)s + X_u \frac{Z_\alpha}{V_o} - \frac{X_\alpha}{V_o} Z_u\right].$$

Whether this polynomial factors into a complex pair as indicated in equation (1) or into two real roots depends on the magnitude of the derivatives X_α and Z_u. Large values of X_α and Z_u tend to produce the complex factors whereas if X_α and Z_u were small, the factors would occur in the more familiar form $(s + 1/T_{\theta_1})(s + 1/T_{\theta_2})$. For the case where $X_\alpha = g$, the factors would be given by $1/T_{\theta_1} = -X_u$ and $1/T_{\theta_2} = -Z_\alpha/V_o$.

Characteristics of short term attitude response which have been found to be important in previous handling qualities studies (References 1, 2, and 3) are the initial pitch rate response per unit control, the steady state pitch rate per unit control deflection or force, the overshoot in pitch rate response, and the long term attitude stiffness and susceptibility to disturbances either from aircraft configuration changes or turbulence. Elements of the $\theta/\delta e$ transfer function (equation 3) which relate to these response characteristics may be observed in the following relationships:

- initial pitch sensitivity, $\frac{\ddot{\theta}}{\delta_c} = K_\delta M_{\delta e} T_\delta$ (4)

- steady state pitch rate sensitivity, $\frac{\dot{\theta}ss}{\delta_c} = K_\delta M_{\delta_e} T'_{sp_1} T'_{sp_2}$ (5)

- pitch rate overshoot, $\frac{\dot{\theta}_{max}}{\dot{\theta}_{ss}} = f\left(T'_{sp_1}/T_\delta \ , \ T'_{sp_2}/T'_{sp_1}\right)$

  as shown in Figure 4.

- attitude stiffness and susceptibility to pitch disturbances,

$$\left(\frac{\Delta\theta}{\Delta M}\right)_{ss} = \frac{\left[N^{\theta}_{\Delta M}\right]_{s\to 0} T'_{sp_1} T'_{sp_2}}{\left(\omega'^2_p\right)} \quad (6)$$

For the pilot evaluations of attitude control during this program, variations were made in T_δ and $T'_{sp1}T'_{sp2}$ in a manner to permit independent evaluations of the initial pitch rate and steady state pitch rate sensitivities. Pitch rate overshoot and attitude stiffness were not independent variables. Overshoot characteristics reflected the variations in $\ddot{\theta}/\delta_c$ and $\dot{\theta}_{ss}/\delta_c$ while attitude stiffness varied primarily as a function of $1/T'_{sp1}T'_{sp2}$. Specific evaluation configurations are described subsequently in this report.

Flight Path and Airspeed Control

Precise control of flight path and airspeed during approach and flare is essential to the achievement of STOL landing field

performance, touchdown sink rates which are acceptable for ride comfort and structural safety considerations, and adequate operating margins for flight safety. Recently published experience with ground based and in-flight simulator evaluations of powered lift jet STOL aircraft (References 4-8) has emphasized the difficulties with path and speed control caused by:

- sluggish flight path response to attitude changes
- operation on the back-side of the thrust required curve
- large changes in lift and drag with engine power setting
- significant coupling between flight path and airspeed with either attitude or power changes
- changes in operating margins with airspeed and angle of attack.

Such behavior implies that significant demands will be placed on the pilot in the way of attention and effort that must be devoted to path and speed control in order to achieve acceptable performance during the approach and landing. Furthermore, it has been evident from this previous work that consistent landing performance and touchdown sink rates have not been achieved even in a research environment. Consequently, it is important to examine the aircraft's behavior so far as flight path and speed response to the pilot's controls are concerned to gain an impression of which response characteristics are likely to be important to the pilot. The discussion which follows describes these response characteristics analytically and identifies the contribution of the aircraft configuration and the flight condition at which it is operated to these response characteristics.

Approximate Response Relationships

The primary controls over path and speed which are assumed in this analysis to be available to the pilot are pitch attitude and engine thrust. When pitch attitude is either tightly controlled by the pilot or is stabilized with a command augmentation system, the aircraft's path and speed response may be described by the following relationships

- response to attitude changes

(a) flight path

$$\left(\frac{\gamma}{\theta_c}\right)_{\theta\rightarrow\delta_e} = \frac{N_{\theta_c}^{\gamma}}{\Delta + Y_\theta N_{\delta_e}^{\theta}}$$

(b) airspeed

$$\left(\frac{u}{\theta_c}\right)_{\theta\rightarrow\delta_e} = \frac{N_{\theta_c}^{u}}{\Delta + Y_\theta N_{\delta_e}^{\theta}} \qquad (7)$$

- response to thrust changes

  (a) flight path (b) airspeed

$$\left(\frac{\gamma}{\delta_T}\right)_{\theta\to\delta_e} = \frac{N^{\gamma}_{\delta_T} + Y_\theta N^{\theta}_{\delta_e}\, N^{\gamma}_{\delta_T}}{\Delta + Y_\theta N^{\theta}_{\delta_e}} \qquad \left(\frac{u}{\delta_T}\right)_{\theta\to\delta_e} = \frac{N^{u}_{\delta_T} + Y_\theta N^{u}_{\delta_T}\, N^{\theta}_{\delta_e}}{\Delta + Y_\theta N^{\theta}_{\delta_e}} \tag{8}$$

for the system represented by the block diagram of Figure 5. It is indicated in Reference 7 that the dominant path and speed response takes place at low frequency, in the region of the root of ω'_p and below. As a consequence, path and speed response at frequencies approaching the closed loop short period may be disregarded for the purpose of approximating the aircraft behavior apparent to the pilot. Such an assumption is justified for path and speed response to attitude by the characteristics illustrated in Figure 6, which are typical of the STOL category of aircraft. These response characteristics may be represented quite adequately by

$$\left(\frac{\gamma}{\theta_c}\right)_{\theta\to\delta_e} \doteq A_{\gamma_\theta}\left(\frac{s + 1/T_{\gamma_\theta}}{s^2 + 2\zeta'_p\omega'_p s + \omega'^2_p}\right) \tag{9}$$

and

$$\left(\frac{u}{\theta_c}\right)_{\theta\to\delta_e} \doteq A_{u_\theta}\left(\frac{s + 1/T_{u_\theta}}{s^2 + 2\zeta_p\omega'_p s + \omega'^2_p}\right) \tag{10}$$

where the numerator roots $1/T_{\gamma\theta}$ and $1/T_{u\theta}$ are the lowest frequency factors of the transfer function numerators $N^{\gamma}_{\theta_c}$ and $N^{u}_{\theta_c}$ and the denominator roots are the closed loop roots associated with the phugoid mode. The same sort of character is exhibited in Figure 7(a) by the path and speed transfer functions to thrust. Contributions of the higher frequency numerator factors and the short period mode are low enough in magnitude to be neglected. Figure 7(b) illustrates the wide separation in frequency of the factors of the path and speed numerators of equations 8(a) and (b) for the value of the attitude loop gain K_θ required to achieve satisfactorily tight attitude control. The thrust transfer functions may thus be approximated by

$$\left(\frac{\gamma}{\delta_T}\right)_{\theta\rightarrow\delta_e} \doteq A_{\gamma_T}\left(\frac{s + 1/T_{\gamma_T}}{s^2 + 2\zeta'_p\omega'_p s + \omega'^2_p}\right) \tag{11}$$

and

$$\left(\frac{u}{\delta_T}\right)_{\theta\rightarrow\delta_e} \doteq A_{u_T}\left(\frac{s + 1/T_{u_T}}{s^2 + 2\zeta'_p\omega'_p\, s + \omega'^2_p}\right) \tag{12}$$

It is now apparent that the path and speed transfer functions to attitude and thrust of equations (9) to (12) appear in the general form

$$\frac{\text{Response}}{\text{Command}} = \frac{A(s + 1/T)}{s^2 + 2\zeta'_p\omega'_p s + \omega'^2_p} \tag{13}$$

with the distinguishing features being the gain A, the numerator root 1/T, and the closed loop phugoid frequency and damping, ω'_p and ζ'_p. Correspondence between these features and a time history of the response to a step command input are shown in Figure 8 where

- the sign of A determines the sign of the initial response
- the relative signs of A and T determine whether the initial and final response are of the same sign
- the magnitude of A and the ratio of $1/T$ to ω_p' determines how quickly the airplane responds initially
- the ratio of $1/T$ to ω_p' determines the amount of overshoot of the response
- the magnitude of $A/T\omega_p'^2$ determines the magnitude of the steady state response.

The wide range of response characteristics illustrated by this example are not generally reflected in the individual path and speed responses. An illustration of path and speed response to attitude and thrust changes for one particular jet STOL configuration is presented in Figure 9a.

The important point to be made is that the flight path and speed response characteristics which typify the STOL aircraft dictate the most effective use of attitude and thrust for control of path and speed on the approach. Considering the response to an attitude change at constant thrust shown in Figure 9, the nose up attitude change produces flight path response typical of that for operation on the backside of the thrust required curve. Path initially shallows but eventually steepens in the long term. Such behavior, as is well known, makes attitude a rather poor control of flight path. However, speed response is conventional, and attitude offers reasonable control over speed providing the harmony between the two is satisfactory. For an increase in thrust with attitude held constant, flight path responds quickly with the long term change determined by specific configuration characteristics. On the other hand speed response is decidedly adverse in that the airplane decelerates for an increase in thrust. Thrust thus appears to be an appropriate control for flight path and a rather poor control for speed.

The preferred control technique is illustrated in the block diagram of Figure 9b. Pitch attitude is stabilized to achieve

good short term attitude response and to suppress the phugoid mode. Tight attitude control can either be accomplished by the pilot or if, as is typical of this category of aircraft, attitude control and stabilization places an excessive burden on the pilot in the presence of other demanding tasks, an attitude command and stabilization capability can be provided by stability augmentation system of the type described previously in this report. With attitude stabilized, airspeed can then be controlled or changes in speed made through changes in the commanded pitch attitude. Flight path tracking is accomplished through changes in thrust. With this control technique specified, the characteristics of the aircraft's response which could conceivably be of importance to the pilot for manual control of the STOL approach and landing may be identified.

Significant Response Characteristics

Considering the example of flight path and airspeed response to thrust shown in Figure 9a, the features which characterize the aircraft's behavior (recalling that thrust is the primary flight path control) are

- the initial response of flight path which indicates how quickly a path correction can be initiated
- the relationship of the long term to short term change in flight path, as illustrated by the amount of overshoot in the response, which indicates how predictably the pilot can make the path correction
- the extent of coupling of speed with flight path, as reflected by the amount of speed change accompanying the change in flight path, which indicates the amount of attention the pilot must devote to path and speed control and the extent to which he must continuously control path and speed closed loop to achieve the precision required for the landing approach.

The response parameters which reflect this behavior are indicated in Figure 10. Initial flight path response is represented by the time constant, τ_γ, which is described by the initial slope, $d\Delta\gamma/dt$, and the peak response $\Delta\gamma_{max}$. Flight path overshoot is reflected in the ratio, $(\Delta\gamma_{max}/\Delta\gamma_{ss})_{\Delta T}$. Flight path-speed coupling is described by the ratio of steady state speed and path changes, $(\Delta u_{ss}/\Delta\gamma_{ss})_{\Delta T}$. Short term speed changes tend to be of small enough magnitude compared to the long term change in speed to be ignored.

Speed control, as was noted previously, is accomplished through changes in pitch attitude. In this case, the steady state speed change for a given change in attitude, $\Delta u_{ss}/\Delta\theta$ is the factor of interest and can be considered a control sensitivity of sorts.

In Figure 11 the contributions to the amount of flight path overshoot can be seen. Whether the characteristic roots of the flight path response are described by $(s^2 + 2\zeta_p'\omega_p's + \omega_p'^2)$ or by $(s + 1/T_{\theta_1}')(s + 1/T_{\theta_2}')$, the significant contribution is the ratio of the numerator root, $1/T_{\gamma T}$, to the lowest frequency characteristic root ω_p' or $1/T_{\theta_1}'$. Of secondary importance is the damping ratio ζ_p' (particularly since ζ_p' tends to be greater than .8 for most attitude loop closures) or the ratio of $1/T_{\theta_1}'$ to $1/T_{\theta_2}'$ (which can fall between the extremes $X_u/(Z_\alpha/V_o) = .1$ when $X_\alpha = 0$ and 1.0 when

$$(X_u + Z_\alpha/V_o)^2 = (4/V_o)(X_u Z_\alpha - X_\alpha Z_u).$$

The amount of overshoot can vary by approximately a factor of five times when the parameters $1/T_{\gamma T}\omega_p'$ or $T_{\theta_1}'/T_{\gamma T}$ vary from .1 to 1.0.

The path response time constant, τ_γ, is defined by

$$\tau_\gamma = \Delta\gamma_{max}/\dot{\gamma}$$

$$= \left(\frac{\Delta\gamma_{max}}{\Delta\gamma_{ss}}\right)_{\Delta T} \left(\frac{\Delta\gamma_{ss}}{\dot{\gamma}}\right)$$

where

$$\frac{\Delta\gamma_{ss}}{\dot{\gamma}} = \frac{Z_{\delta_T}\left(1/T_{\gamma_T}\omega_p'^2\right)}{Z_{\delta_T}}$$

$$= 1/T_{\gamma_T}\omega_p'^2$$

and thus

$$\tau_\gamma = \left(\frac{\Delta\gamma_{max}}{\Delta\gamma_{ss}}\right)_{\Delta T} \left(\frac{1}{T_{\gamma_T}\omega_p'^2}\right) \tag{14}$$

Therefore, the initial time response is dependent both on the ratio $1/T_{\gamma_T}\omega_p'$, which defines the path overshoot characteristics, and the characteristic frequency, ω_p'.

Flight path-speed coupling can be derived from the steady state path and speed response to thrust given by equations (11) and 12), i.e.,

$$\left(\frac{\Delta u_{ss}}{\Delta\gamma_{ss}}\right)_{\Delta T} = \left(\frac{A_{u_T}}{T_{u_T}\omega_p'^2}\right)\left(\frac{T_{\gamma_T}\omega_p'^2}{A_{\gamma_T}}\right)$$

$$= \left(\frac{A_{u_T}}{A_{\gamma_T}}\right)\left(\frac{T_{\gamma_T}}{T_{u_T}}\right) \tag{15}$$

where the individual terms as described in Reference 7 are,

$$A_{u_T} = X_{\delta_T} \tag{16}$$

$$A_{\gamma_T} = -\frac{Z_{\delta_T}}{V_o} \tag{17}$$

$$1/T_{u_T} \doteq -\frac{Z_\alpha}{V_o} + \frac{X_\alpha}{V_o}\frac{Z_{\delta_T}}{X_{\delta_T}} \tag{18}$$

$$1/T_{\gamma_T} \doteq - X_u + Z_u \frac{X_{\delta_T}}{Z_{\delta_T}} \tag{19}$$

$$\omega_p'^2 \doteq X_u \frac{Z_\alpha}{V_o} - Z_u \frac{X_\alpha}{V_o} \tag{20}$$

With suitable manipulation, equation (15) may be rewritten as

$$\left(\frac{\Delta u_{ss}}{\Delta \gamma_{ss}}\right)_{\Delta T} = \frac{T_{\gamma_T} \omega_p'^2}{Z_u/V_o} \left[1 + \left(\frac{1}{T_{\gamma_T} \omega_p'^2}\right) \frac{Z_\alpha}{V_o}\right] \tag{21}$$

It is a function of $1/T_{\gamma_T}\omega_p'$, both of which enter into the definition of $(\Delta\gamma_{max}/\Delta\gamma_{ss})_{\Delta T}$ and τ_γ, and also of the linear perturbation derivatives Z_u and Z_α. Hence the extent that flight path-speed coupling can vary independently of the flight path response to thrust is determined by the magnitude of the Z axis derivatives due to speed and angle of attack.

Speed sensitivity to attitude changes is simply the steady state magnitude of equation (10), i.e.,

$$\frac{\Delta u_{ss}}{\Delta \theta} = \frac{A_{u_\theta}}{T_{u_\theta} \omega_p'^2} \tag{22}$$

where

$$A_{u_\theta} = X_\alpha - g \tag{23}$$

$$1/T_{u_\theta} \doteq \frac{Z_\alpha}{V_o} \left(\frac{g}{X_\alpha - g}\right) \tag{24}$$

as derived in Reference 7. Thus equation (22) becomes

$$\frac{\Delta u_{ss}}{\Delta\theta} = g\left(\frac{Z_\alpha}{V_o}\right)\left(\frac{1}{\omega_p'^2}\right) \tag{25}$$

and if $X_\alpha = 0$, so that $\omega_p'^2 \doteq X_u(Z_\alpha/V_o)$,

then $\Delta u_{ss}/\Delta\theta \doteq g/X_u$.

Contributions of Aircraft Configuration and Flight Condition

Considering the contributions to the flight path and speed control characteristics shown respectively in Figure 11 and equations (14), (21), and (25), the dominant factors which appear are $1/T_{\gamma T}\omega_p'$, ω_p', Z_u and Z_α/V_o. The perturbation derivatives which define the path numerator root, $1/T_{\gamma T}$, and the closed loop phugoid frequency, ω_p', are shown in equations (19) and (20) to be X_u, X_α, Z_u, Z_α, and $X_{\delta_T}/Z_{\delta_T}$. Thus, the significant flight path and speed response characteristics to thrust and attitude control are defined in terms of the aircraft's X and Z axis (or drag and lift) derivatives due to speed, angle of attack, and thrust. Reference 9 shows that these derivatives may be described in terms of the vehicle configurations and flight condition, i.e.,

- X_u - axial velocity damping; a function of drag coefficient, trim airspeed, and wing loading (may be augmented by autospeed control)
- X_α - drag due to lift; a function of trim airspeed, wing loading, and induced drag
- Z_u - vertical force coupling with axial velocity; a function of trim airspeed
- Z_α - vertical velocity damping; a function of lift curve slope, trim airspeed, and wing loading
- $X_{\delta_T}/Z_{\delta_T}$ - effective trust line inclination $\theta_T = \cot^{-1}\left(-X_{\delta_T}/Z_{\delta_T}\right)$

These characteristics are determined for all practical purposes by the flight condition at which the aircraft is being operated, by its wing loading, and by the efficiency of its high lift system. Thus, when landing field length (approach speed), cruise Mach number (wing loading), and high lift system design are selected, the aircraft's behavior as it appears to the pilot flying the approach and landing will be essentially determined.

EXPERIMENTAL PROGRAM

Description of the Simulation

A ground based flight simulation of a powered lift jet STOL aircraft was used as a basis for piloted evaluation of the pitch attitude, flight path, and airspeed response characteristics described in the previous section of this report. The simulation facility utilized was the Ames Research Center Flight Simulator for Advanced Aircraft (FSAA), a large motion facility with a high resolution visual display as described in Reference 10. The vehicle on which the simulation was based was the Augmentor Wing Research Aircraft, a modified DeHavilland of Canada C-8A Buffalo airframe incorporating an augmentor flap system for generating high lift coefficients for high wing loading STOL operation and deflected hot thrust to permit operation on steep flight paths. The aircraft is described in Reference 11. A real time digital model of the aircraft's non-linear aerodynamics and its flight control system were programmed as described in Reference 12 for the XDS-Sigma 8 computer dedicated to the FSAA facility. The static aerodynamic characteristics were derived as shown in Reference 13 from model tests of the vehicle in the Ames 40 × 80 foot wind tunnel. Rotary derivatives were estimated using jet flap theory where appropriate. Supporting data for these derivatives are unpublished although the models themselves appear in Reference 13. Jet engine acceleration-deceleration characteristics were modeled to represent the results shown in Reference 13.

The longitudinal flight control system provided for pitch axis command augmentation and alteration of the vehicle's longitudinal force characteristics through the use of vectored thrust. Pitch control was accomplished through the aircraft's existing elevator-spring tab system. Augmentation commands were provided in series with the pilot's control column inputs. Longitudinal force control was achieved by vectoring the engines'

hot thrust about a trim position deflected 90 degrees to the approach path. Thrust vectoring was accomplished by driving the engine's exhaust nozzles with commands composed of airspeed, angle of attack, and throttle position error signals. For thrust vectoring of ±15 degrees about the 90 degree trim condition, effective alteration of the basic aircraft's X_u, X_α, and X_{δ_T} derivatives was possible with no corresponding contribution of any consequence to the Z axis force characteristics. A block diagram of the longitudinal control system is shown in Figure A4 of the Appendix.

Test Program

Pitch attitude control was evaluated using the pitch rate command/attitude hold system described previously in the report and shown in Figure 1. A matrix of the test configurations is presented in Table 1. A description of the basic Augmentor Wing aircraft, in terms of its stability derivatives, characteristics modes, pertinent transfer function numerator factors, and transient response characteristics is provided in the Appendix. The dynamics of the elevator-spring tab system are documented in that description.

Flight path and airspeed control evaluations were performed using the control technique described in Figure 9. Variations in each of the path and speed response characteristics previously described were achieved through variations in the longitudinal force characteristics X_u, X_α, and X_{δ_T}. The contributions of these derivatives are described by equations (19) and (20) and are shown in Figures 12 and 13. Effects of variation in thrust inclination (θ_T) and drag due to lift (X_α) are shown in Figure 12 for characteristics otherwise representative of the basic aircraft. In Figure 13, the influence of axial damping (X_u) in combination with thrust inclination is shown. A summary of the significant interaction of these derivatives with the response characteristics is presented in Table II.

Sets of configurations were selected to permit independent evaluations of the path response time constant τ_γ and the speed response to attitude $\Delta u_{ss}/\Delta\theta$ for minimal path overshoot and path-speed coupling. It was also possible to evaluate both the overshoot and coupling parameters independently of the effects of initial path response to thrust or speed response to attitude. As can be appreciated from the trends of the overshoot and coupling parameters in Figures 12 and 13, it was not possible to evaluate them independently of each other when only X_u, X_α, or θ_T were varied. This point is demonstrated more conclusively in Figure 14,

by a collection of configurations from Figures 12 and 13 having common values of X_u, X_α, and θ_T. The correlation between path overshoot and path-speed coupling in the region

$$\left(\frac{\Delta\gamma_{max}}{\Delta\gamma_{ss}}\right)_{\Delta T} > 1.3$$

$$\left(\frac{\Delta u_{ss}}{\Delta\gamma_{ss}}\right)_{\Delta T} < -1.0 \text{ knots/deg}$$

is quite strong and is implicit in relationship described by equation (21), where for constant values of Z_u or Z_α as shown in Figure 12, both the overshoot and coupling parameters are dominated by the term $1/T_{\gamma_T}\omega_p'$. Variation of either of the derivatives Z_u or Z_α could provide for independent variation in path overshoot or path-speed coupling, although neither of these derivatives was altered in the test program. The range over which the overshoot and coupling characteristics could be considered independent for variations in Z_u or Z_α is indicated in Figure 14. The region of practical importance to powered lift STOL as determined by wing loading and approach speed is crosshatched in the figure. Evaluations of test configurations from among those spotted in the region by the solid symbols gave an appreciation of the contribution of these characteristics to handling qualities for path and speed control on the approach.

Specific test configurations for the evaluations are listed in Table III. Response parameters with their corresponding transfer function factors and stability derivatives are compiled therein. A suitable pitch rate command/attitude hold configuration was implemented to reduce the pilot's pitch axis control workload. The characteristics of this system are indicated in Figure A4 of the Appendix.

Evaluation Task and Experimental Data

For the approach and landing, the pilot assumed control of the aircraft with it trimmed and configured for descent on the glideslope and aligned with the localizer. The approach was made

to a 1500 foot STOL runway, with touch down zone markings as indicated in Figure 15. The aircraft was trimmed at 1300 feet for descent on a 7.5 degree glideslope at an airspeed of 60 knots. Flaps were set at 65 degrees, hot thrust was vectored 90 degrees to the aircraft's reference waterline, and power was set corresponding to 6380 pounds of hot thrust. Lateral-directional stability augmentation, including roll damping, spiral mode stabilization, Dutch roll damping, and turn coordination, was utilized to improve control of bank angle, heading, and sideslip to prevent these factors from influencing the pilot's evaluation.

Two Ames experimental test pilots participated in the program. During the approach, the pilots introduced their own disturbances, offsets, and abuses as a means of evaluating each configuration. Both VFR and IFR evaluations were performed. Approach guidance was provided by raw ILS glideslope and localizer error information. Time histories of the aircraft's response and the pilot's control activity were recorded. Average values and standard deviations were computed over separate altitude intervals of 1300 to 300 feet and 300 to 50 feet for

pitch attitude	normal acceleration at c.g.	control column displacement
pitch rate	vertical velocity	throttle displacement
airspeed	glideslope error	

Touchdown status information was recorded for

pitch attitude	distance from runway threshold
angle of attack	sink rate
airspeed	

Pilot opinion ratings and commentary based on the Cooper-Harper scale described in Reference 14, were obtained for each configuration with regard to its handling qualities during the approach. Separate ratings for the landing flare were not obtained on a consistent basis; however specific comments on the aircraft's handling during the flare as compared to the approach were noted.

DISCUSSION OF RESULTS

In the discussion to follow, pilot's evaluations of pitch attitude, flight path and airspeed control will be presented for the landing approach. Pilot ratings will specifically apply to this portion of the task. Separate commentary on landing flare characteristics will be included in a section at the end of this discussion.

Pitch Attitude Control

Features of the pitch rate command system which were evaluated were the initial pitch rate response sensitivity and the steady state pitch rate control sensitivity. The test configurations are illustrated in the root locus and frequency response plots of Figure 16. Variations in magnitude of the transfer functions at high frequency provide a range in the initial pitch sensitivity of $\ddot{\theta}/\delta_c$ = .05 to .21 rad/sec^2 per inch of column. Variations in steady state pitch rate sensitivity which accompany the different levels of low frequency gain are $\dot{\theta}_{ss}/\delta_c$ = 1.5 to 3.8 deg/sec per inch of column.

Pilot ratings for these configurations are presented in Figure 17. They are plotted in the upper diagram against initial response sensitivity for varying levels of pitch rate sensitivity. The pilot's preference for initial pitch sensitivity lies in the neighborhood of $\ddot{\theta}/\delta_c$ = .1 rad/sec^2 per inch, with steady pitch rate sensitivity on the order of $\dot{\theta}_{ss}/\delta_c$ = 2.0 deg/sec per inch. Reductions or increases either in the initial or steady state pitch rate sensitivities from either of these values produce moderate degradations in pilot rating. Pitch rate overshoot does not appear as an independent variable in these configurations. The relationship of the overshoot ratio to the initial and steady state control sensitivities is reflected in the lower diagram of Figure 17 with $\dot{\theta}_{max}/\dot{\theta}_{ss}$ varying from 1.0 to 1.5.

Pilot commentary, which is summarized in Figure 18, indicates objections to abrupt pitch response which characterize the configurations with the lower $T'_{sp1}T'_{sp2}/T_\delta$ ratios; that is the highest sensitivity configurations. The contrast in initial response characteristics is evident in the sample of time histories of the figure for variations in $1/T_\delta$ and $1/T'_{sp1}T'_{sp2}$. Configurations with higher $T'_{sp1}T'_{sp2}/T_\delta$ ratios were noted to be somewhat sluggish in response to the pilot's control input. Initial response characteristics of the lowest frequency configurations were satisfactory. However, their susceptability to upset from pitching moment disturbances from power or configuration changes or turbulence made them somewhat objectionable overall.

In summary, the most favorable characteristics of the pitch rate command system are represented by closed loop roots corresponding to $1/T'_{sp1}T'_{sp2}$ = 2.8 and a first order lead which gives $T'_{sp1}T'_{sp2}/T_\delta$= .35. The corresponding pitch response characteristics are

$$\frac{\ddot{\theta}}{\delta_c} = .1 \text{ rad/sec}^2 \text{ per inch}$$

$$\frac{\dot{\theta}_{ss}}{\delta_c} = 2.0 \text{ deg/sec per inch}$$

The pitch axis command and stabilization system utilized for the subsequent flight path and airspeed control investigation provided these characteristics and was identical to Configuration 1 of Table I.

Flight Path and Airspeed Control

At the outset of this discussion, the influence of flight path and airspeed response to thrust will be considered, with attention given first to the effect of initial flight path response. Pilot ratings are shown in Figure 19 for a range of flight path time constants, (τ_γ). The results are presented for minimal values of flight path overshoot and flight path speed coupling, i.e., essentially no overshoot or coupling existed for these configurations. A wide range of flight path-velocity trim conditions were included in these configurations, ranging from an extreme backside of the thrust required curve ($d\gamma/dV$ =.47 deg/knot to an extreme frontside case ($d\gamma/dV$ = -1.23 deg/knot). Pilot ratings appear to be insensitive to variations in τ_γ over the range of configurations tested. The results are understandable in light of the evaluation task. During the approach, extremely rapid path corrections are not required and, as the pilots indicate, can readily be made for the various configurations shown in Figure 19. As indicated in Reference 15, bandwidths required for closed loop path control are on the order of .5 to 1.0 radians/second. For these configurations, and with the effects of engine acceleration-deceleration included, the required path control bandwidths can be achieved with little demand for compensation placed on the pilot.

Scatter in these pilot rating data are somewhat more than $\pm$1/2 rating unit which has come be be expected from experienced evaluation pilots. If the scatter is anything other than random in origin, it is likely to be due to a moderate influence of the range of flight path-velocity ($d\gamma/dV$) characteristics included in these configurations. In fact, the pilots' commentary showed dissatisfaction with the extreme backside or frontside configurations ($d\gamma/dV$ = .47 or -1.23 deg/knot) due to the excessive speed

sensitivity to attitude changes of the former and insensitivity of speed to attitude of the latter. In neither case did any consideration of the stability of flight path control with attitude arise to influence the pilots' ratings.

It should be noted that these configurations were evaluated for an optimized throttle sensitivity of $Z_{\delta T} = -.08$ g's/inch. No variations in Z axis characteristics were made for the various configurations. Although an increase in vertical velocity damping (Z_α/V_o) could quicken the initial path response, it was not evaluated in this program. As will be indicated subsequently in the discussion of flare characteristics, some quickening of path response such as could be achieved through Z_α augmentation would be beneficial to flare control.

Flight path overshoot ($\Delta\gamma_{max}/\Delta\gamma_{ss}$) and flight path-speed coupling ($\Delta u_{ss}/\Delta\gamma_{ss}$) are two characteristics of response to thrust which, as has been previously noted, could not be evaluated independently in this program. They are strongly interrelated due to their mutual sensitivity to changes in longitudinal (X-axis) force characteristics such as trimmed drag, drag due to lift, and thrust inclination. However, this interrelationship is typical of powered lift STOL aircraft in general as was shown in Figure 14 and the evaluation of mutual changes in these two parameters which was conducted in this program offers insight into their influence on path and speed control for this category of aircraft. Results are presented in Figure 20, with pilot ratings plotted against the path-speed coupling parameter $(\Delta u_{ss}/\Delta\gamma_{ss})_{\Delta T}$. The path-speed coupling influence was identified by the pilots as the primary contribution to their evaluation and rating and hence was felt to be the relevant parameter for interpreting the data.

It is apparent that path-speed coupling has a pronounced effect on pilot ratings of path-speed control. In particular a significant degradation in ratings can be noted for values of $(\Delta u_{ss}/\Delta\gamma_{ss})_{\Delta T}$ in excess of -3 knots/degree. The adverse nature of the speed response to a flight path change with thrust is illustrated in the inset diagram at the left of the figure, where an increase in thrust to shallow the path causes the aircraft to decelerate, in turn washing out the intended path correction. Such behavior is particularly undesirable in that the strongly coupled response demands that the pilot pay considerable attention to path and speed control and to work in a continuous, coordinated, closed-loop fashion with attitude and thrust to achieve adequate precision of path and speed control. Furthermore, the attitude control technique required for holding

speed constant while making a path correction with thrust is unnatural. It requires the pilot to lower the nose to hold speed while attempting to climb and vice-versa. For these two reasons, strong path-speed coupling can make the aircraft unacceptable for flying the STOL approach.

To conclude the discussion of path and speed control for the approach it is necessary to determine the significance of speed behavior in response to its primary control, pitch attitude. The parameter for evaluation is the steady speed change in response to a change in pitch attitude ($\Delta u_{ss}/\Delta\theta_c$). It should be clear from the relationships associated with equation (25) that speed response to attitude and path-velocity ($d\gamma/dV$) characteristics are strongly related through their mutual dependence on the level of **trimmed drag and drag due to** lift. This interrelation was brought out in the peripheral discussion related to Figure 19 and the initial flight path response. The interrelationship is one which provides for large speed changes with attitude for operation on the backside of the thrust required curve and small speed changes with attitude for frontside operation. For the control technique utilized in these simulation evaluations of path and speed response (speed control with attitude, path control with thrust) considerations related to speed response to attitude **appears to be more important than the degree of frontside or backside operation involved.**

The significance of speed control with attitude is indicated in Figure 21. Pilot ratings for variations in the speed response parameter $\Delta u_{ss}/\Delta\theta$ are plotted for otherwise favorable values of τ_γ and $(\Delta u_{ss}/\Delta\gamma_{ss})_{\Delta T}$. Variations in speed sensitivity to attitude have only a modest effect on pilot ratings. As might be expected the pilots objected, although not too strongly, to insensitive or to excessively sensitive speed response to attitude changes. Poor harmony between speed and attitude either required objectionably large attitude changes for ordinary speed control or an unnecessarily fine touch on attitude with attitude changes to avoid objectionable speed excursions. Proper harmony seems to dictate a speed-attitude sensitivity on the order of $\Delta u_{ss}/\Delta\theta$ between -1.5 and -2.5 knots per degree.

Flare Control

The pilots did not specifically evaluate the flare maneuver as distinct from the landing approach. However, specific comments were made on flare characteristics where appropriate and it is on these comments that the following discussion is largely based.

First of all it is evident from the results of this program as well as for those reported in References 4, 5, 6, and 8 that the two-control flare (that is where thrust is used to augment the flare with attitude) does not produce consistent STOL landing performance, either in terms of touchdown precision or low sink rates. A compilation of data of landing precision in terms of sink rate and point of touchdown for all of the configurations evaluated in this program is presented in Figure 22. It should be mentioned that these data were obtained from experimental runs where the pilot's objective was to achieve the best landing performance possible rather than to carry out an evaluation of the aircraft's handling qualities. The pilots sought to land the aircraft within the touchdown zone and if possible at a sink rate of 6 ft/sec or less. The scatter in landing precision data of Figure 22 speaks for itself. Touchdown sink rates, with one exception, exceeded 5 ft/sec and most landings were made at sink rates from 8 to 10 ft/sec. Separation of the data into sets of configurations which could isolate effects of flight path time constant and speed response to attitude (which includes the influence of frontside or backside operation) offers no further enlightenment. Data is presented in this form in Figure 23, and there are no discernible trends present for landing precision, touchdown sink rate or airspeed.

It can be questioned whether STOL operation is or should be compatible with minimizing sink rate at touchdown. The conceivable bounds for sink rate probably lie somewhere between a 3 ft/sec lower limit comparable to CTOL operation and a 12 to 14 ft/sec upper limit defined by the nominal approach path angle and airspeed. Without attempting to place the results of this program in an acceptable or unacceptable category as regards landing impact, it can be said that landings performed on the simulator have produced sink rates somewhere half way between these two limits. These results should be qualified by the ground effects due to high lift included in the simulation. As noted in Reference 12, ground effects at touchdown produce a 5 percent reduction in drag and a 12 percent reduction in lift for the nominal approach condition.

It should be emphasized that the problem of achieving accurate landings at low sink rates does not stem from a lack of capability of the basic aircraft; that is, the capability for generating the normal load factors to curve the flight path to terminate the approach at the proper position and vertical velocity. The potential for generating normal acceleration (Δa_z) is more than adequate if aircraft rotation and an increase in power are both used. Instead, the problem is one of control of this load factor and how to generate it quickly and precisely to permit a precision flare to be made. In this program, no sophisticated control schemes were investigated for

flare, such as control interconnects (e.g. column to throttles or Z_α augmentation). The basic aircraft's controls for short term flight path changes were evaluated and, as with the other referenced powered lift STOL simulations, they were found to be inadequate for the task.

Second, it should be apparent that path and speed control characteristics which are favorable for the approach are not necessarily favorable for control through the flare to landing. In particular, flight path response time constants which have been shown in Figure 19 to be satisfactory for the approach do not permit path corrections to be accomplished quickly enough for the flare. A sample time history of an STOL landing is presented in Figure 24 for the configuration having the best path and speed control characteristics for the approach. The time frame for the flare, from the point at which the pilot initiates the maneuver with the elevator to touchdown, is 3 seconds. For any control to be useful for path corrections within this time frame, the corrections must be initiated and stabilized within approximately 2 seconds. Such response implies equivalent first order time constants on the order of .75 to 1.0 seconds. Neither the dynamics of the basic airframe, which responds at frequencies on the order of ω_p' to either attitude or thrust changes, or the engine dynamic response, which requires 1.5 to 2.0 seconds to stabilize following a commanded thrust change, offers the kind of response demanded. Clearly a need exists for utilizing the potential existing in the basic aerodynamics and reserve thrust to achieve the desired flare capability. The solution most likely lies with quickened engine acceleration characteristics and augmentation of the aircraft's vertical velocity damping Z_α/V_o. So far as speed response and control is concerned, it could be speculated that the characteristics of speed response to thrust which were judged adverse for the approach may not be so objectionable for the flare. The time span over which the speed change can occur does not allow for significant changes in speed considering the speed response time constants involved. However, speed response to attitude is likely to be important to the pilot in order that he can rely on a reasonable and predictable speed bleed off through the flare to touchdown.

The third point to be made is that the successful use of two controls to accomplish the flare demands that one of the controls be identified as primary and the other control be relegated to a secondary or supporting role. Throughout this program and during other STOL simulations at Ames as well, the evaluation pilots virtually unanimously expressed a preference

for a single control with which to perform the flare. Their motivation was the desire to simplify the flare technique so as to be able to get consistent results in real operational use. If a single control cannot be devised* and, as a result, two controls must be used, the pilots would prefer to be able to initiate the flare with the primary control and to use it for flight path corrections as required throughout the flare. The primary control could either be attitude or power and it should have the quick time response previously indicated. The secondary control would be used in an open-loop or pre-programmed manner to assist the flare and would not be used further to perform corrections to the flare. As the pilots indicate, they cannot simultaneously use two controls in a closed loop fashion to accomplish the flare and at the same time have confidence in their ability to get consistently good landing performance.

It must be borne in mind that the ability to satisfactorily produce the motion and visual cues crucial to the pilot for performing this maneuver is always in question when a ground based simulator is used. Notwithstanding the motion capability of the FSAA and the visual resolution capability of the Redifon system, the evaluation pilots harbored doubts of their ability to judge altitude, sink rate, and normal acceleration and to use these cues effectively in controlling the aircraft through the flare. However, even with these qualifications of the experimental results, it is felt that their interpretation for the purpose of distinguishing between significant and inconsequential contributions to the flare and landing is valid.

CONCLUSIONS

The conclusions which can be drawn from the experimental program are qualified where appropriate by the technique used by the pilot to control flight path and airspeed during the landing approach. Further qualification of the results obtained for the landing flare are imposed by the ability to adequately reproduce the motion and visual cues important to the pilot for performing this maneuver.

---

*The control must also be suitable for use during the approach and for wave-offs, for adapting to engine failures, and at the same time be highly reliable and easily maintained.

With these qualifications, the following conclusions can be made as a result of the analytical and simulation studies of pitch attitude, flight path, and airspeed control for powered lift STOL aircraft.

- Satisfactory pitch attitude control can be achieved with a pitch rate command/attitude hold system which has the following characteristics:

  initial pitch response sensitivity = .1 rad/sec^2 per inch

  steady pitch rate sensitivity = 2.0 deg/sec per inch

- With pitch attitude stabilized and for flight path control with thrust and airspeed control with pitch attitude, the characteristics which define path and speed response as they appear to the pilot are

  initial flight path time constant in response to thrust

  overshoot in flight path response to thrust

  flight path-speed coupling defined by the change in speed following a path correction with thrust

  speed change due to a change in attitude.

  Following the approach of Reference 7, these path and speed response characteristics can be defined in terms of the following configuration and flight condition dependent characteristics

  axial velocity damping - X_u and Z_α/V_o

  axial velocity coupling - X_α and Z_u

  effective thrust inclination - $X_{\delta_T}/Z_{\delta_T}$.

- For flight path and airspeed control during the approach and over a range of configuration characteristics appropriate to powered lift STOL

  flight path-airspeed coupling is the dominant influence on handling qualities

  speed sensitivity to pitch attitude has a moderate influence on handling qualities

initial flight path time constant has a negligible effect over the range investigated ($1.5 < \tau_{\gamma} \pm < 7$ sec).

- Favorable or unfavorable flare control characteristics are not necessarily compatible with control characteristics desired for the approach. The ability to draw firm conclusions regarding desirable flare characteristics is restricted by the quality of the flare simulation. Nevertheless, it is likely that

  compared to flight path control on the approach, quicker flight path response will be required to achieve the landing precision required for STOL field lengths and touchdown sink rates less than 6 ft/sec

  more sophisticated control schemes, such as control integration and vertical velocity damping augmentation, will be required to realize the inherent potential of the basic aircraft's aerodynamics and reserve thrust for performing the flare.

REFERENCES

1. Chalk, C. R., Neal, T. P., Harris, T. M., Pritchard, F. E. and Woodcock, R. J., Background Information and User Guide for MIL-F-8785B(ASG), "Military Specification-Flying Qualities of Piloted Airplanes," AFFDL-TR-69-72, August 1969.

2. Chalk, C. R., Key, D. L., Kroll, J., Wasserman, R. and Radford, R. C., Background Information and User Guide for MIL-F-83300, "Military Specification-Flying Qualities of Piloted V/STOL Aircraft," AFFDL-TR-70-88, November 1970.

3. Stapleford, R. L. and Ashkenas, I. L., Analysis of Several Handling Quality Topics Pertinent to Advanced Manned Aircraft: Longitudinal Short-Period Handling Quality Requirements, AFFDL-TR-67-2, June 1967.

4. Franklin, J. A. and Innis, R. C., Longitudinal Handling Qualities During Approach and Landing of a Powered Lift STOL Aircraft, NASA TMX-62,144, March 1972.

5. Grantham, W. D., Nguyen, L. T., Patton, J. M., Deal, P. L., Champine, R. A. and Carter, C. R., Fixed Base Simulator Study of an Externally Blown Flap STOL Transport Airplane During Approach and Landing, NASA TN-D-6898, October 1972.

6. Hassell, J. L. and Judd, J. H., Study of Ground Proximity Effects on Powered Lift STOL Landing Performance, Proceedings of the NASA STOL Technology Conference, Ames Research Center, October 17-19, 1972.

7. Craig, S. J., Ashkenas, I. L., and Heffley, R. K., Pilot Background and Vehicle Parameters Governing Control Technique in STOL Approach Situations, Report No. FAA-RD-72-69, June 1972, Federal Aviation Administration.

8. Allison, R. L., Mack, M., and Rumsey, P. C., "Design Evaluation Criteria for Commercial STOL Transports," NASA CR-114454, June 1972.

9. Seckel, E., Stability and Control of Airplanes and Helicopters, Academic Press, New York, 1964.

10. Zuccaro, J. L., The Flight Simulator for Advanced Aircraft - A New Aeronautical Research Tool, AIAA Paper 70-359, March 1970.

11. Quigley, H. C., Sinclair, S. R. M., Nark, T. C. and O'Keefe, J. V., A Progress Report on the Development of an Augmentor Wing Jet STOL Research Aircraft, SAE Paper 710757, National Aeronautics and Space Engineering and Manufacturing Meeting, Los Angeles, Calif., Sept. 28-30, 1971.

12. Cleveland, W. B., Vomaske, R. F. and Sinclair, S. R. M., Augmentor Wing Jet STOL Research Aircraft Digital Simulation Model, NASA TMX-62,149, April 1972.

13. Rumsey, P. C. and Spitzer, R. E., Simulator Model Specification for the Augmentor Wing Jet STOL Research Aircraft, NASA CR-114434, December 1971.

14. Cooper, G. E. and Harper, R. P., The Use of Pilot Rating in the Evaluation of Aircraft Handling Qualities, NASA TN D-5153, April 1969.

15. Ashkenas, I. L. and Craig, S. J., Multiloop Piloting Aspects of Longitudinal Approach Path Control, Paper presented at the 8th Congress of International Council of Aeronautical Sciences, Amsterdam, August 28 - September 2, 1972.

TABLE I

PITCH RATE COMMAND/ATTITUDE HOLD CONFIGURATIONS

Config	K_δ deg/in	T_δ sec	K_θ deg/deg	$\frac{K_q}{\frac{deg}{deg/sec}}$	ζ_p'	ω_p' rad/sec	$\frac{1}{T'_{sp_1}}$ rad/sec	$\frac{1}{T'_{sp_2}}$ rad/sec	$\frac{\ddot{\theta}/\delta_c}{\frac{rad/sec^2}{inch}}$	$\frac{\dot{\theta}_{ss}/\delta_c}{\frac{deg/sec}{inch}}$	$\frac{\dot{\theta}_{max}}{\dot{\theta}_{ss}}$
1	-5.	1.0	-2.	-2.	.94	.27	.93	2.99	.105	2.2	1.0
2	-5.	.5	-2.	-2.	.94	.27	.93	2.99	.05	2.2	1.0
3	-5.	2.0	-2.	-2.	.94	.27	.93	2.99	.21	2.2	1.45
4	-5.	1.0	-3.	-3.	.98	.27	.96	4.10	.105	1.5	1.0
5	-7.5	1.0	-3.	-3.	.98	.27	.96	4.10	.16	2.3	1.0
6	-5.	.5	-3.	-3.	.98	.27	.96	4.10	.05	1.5	1.0
7	-5.	2.0	-3.	-3.	.98	.27	.96	4.10	.21	1.5	1.5
8	-5.	1.0	-1.	-1.	.82	.28	.86	1.85	.105	3.8	1.0
9	-5.	2.0	-1.	-1.	.82	.28	.86	1.85	.21	3.8	1.3

$\delta_{c_{breakout}} = \pm .5$ inch

TABLE II

CONTRIBUTIONS TO FLIGHT PATH AND AIRSPEED RESPONSE CHARACTERISTICS

(a) $\theta_T > 80$ degrees

Derivative	Response Characteristic			
	τ_γ	$\left(\frac{\Delta\gamma_{max}}{\Delta\gamma_{ss}}\right)_{\Delta T}$	$\left(\frac{\Delta u_{ss}}{\Delta\gamma_{ss}}\right)_{\Delta T}$	$\frac{\Delta u_{ss}}{\Delta\theta}$
X_α	Minimal	Large	Large	Large. Independent of θ_T
X_u	Minimal	Large	Large	Moderate. Independent of θ_T

(b) $45 < \theta_T < 80$ degrees

Derivative	Response Characteristic			
	τ_γ	$\left(\frac{\Delta\gamma_{max}}{\Delta\gamma_{ss}}\right)_{\Delta T}$	$\left(\frac{\Delta u_{ss}}{\Delta\gamma_{ss}}\right)_{\Delta T}$	$\frac{\Delta u_{ss}}{\Delta\theta}$
X_α	Large	Minimal	Moderate	Large. Independent of θ_T
X_u	Moderate	Minimal	Minimal	Moderate. Independent of θ_T

TABLE III

CONFIGURATIONS FOR FLIGHT PATH AND AIRSPEED CONTROL

Config	X_u 1/sec	$\frac{X_\alpha}{V_o}$ 1/sec	$\frac{X_{\delta_T}}{Z_{\delta_T}}$	$\zeta'_p \left(1/T'_{\theta_1}\right)$	$\omega'_p \left(1/T'_{\theta_2}\right)$	γ/δ_T		u/δ_T		τ_γ sec	$\left(\frac{\Delta\gamma_{max}}{\Delta\gamma_{ss}}\right)_{\Delta T}$	$\left(\frac{\Delta u_{ss}}{\Delta\gamma_{ss}}\right)_{\Delta T}$ knots/deg	$\left(\frac{\Delta u_{ss}}{\Delta\theta}\right)$ knots/deg
						$\frac{1}{T_{\gamma_T}}$ rad/sec	γ_{ss}/δ_T rad/lb	$\frac{1}{T_{u_T}}$ rad/sec	u_{ss}/δ_T ft/sec/lb				
1	-.052	.14	-.16	.94	.27	.10	.0024	-.52	-.002	1.81	1.3	-.83	-2.2
2	-.052	.14	-.3	.94	.27	.15	.0034	-.07	-.0005	2.37	1.2	-.15	-2.2
3	-.052	.14	-.56	.94	.27	.23	.0052	.17	.0021	3.16	1.05	.42	-2.2
4	-.052	.14	-.91	.94	.27	.34	.0076	.28	.0058	4.5	1.0	.76	-2.2
5	-.052	.3	-.62	.73	.34	.24	.0034	-.05	-.0004	2.45	1.2	-.12	-1.4
6	-.052	.3	-.91	.73	.34	.33	.0047	.11	.0015	3.09	1.1	.31	-1.4
7	-.2	0.	-.32	(.26)	(.43)	.32	.005	.39	.0018	2.89	1.0	.37	-1.5
8	-.052	.14	.11	.94	.27	.021	.0005	2.34	-.0048	1.39	5.0	-10.0	-2.2
9	-.052	.14	-.02	.94	.27	.062	.0014	-6.37	-.0034	1.57	1.9	-2.4	-2.2
10	-.052	.3	-.02	.73	.34	.058	.0008	-13.7	-.0043	1.49	3.0	-5.1	-1.4
11	-.052	.3	-.32	.73	.34	.149	.0021	-.51	-.0024	1.89	1.5	-1.11	-1.4
12	-.052	0.	-.02	(.08)	(.44)	.065	.0032	-.71	-.0008	2.02	1.1	-.26	-4.6
13	-.052	0.	-.32	(.08)	(.44)	.16	.0076	.39	.0058	4.42	1.0	.76	-4.6
14	-.052	0.	-.62	(.08)	(.44)	.25	.012	.42	.0124	7.02	1.0	1.03	-4.6
15	-.2	.14	-.32	.87	.38	.32	.0036	-.043	-.0002	2.36	1.1	-.04	-1.1
16	-.5	.14	-.02	.91	.54	.54	.0032	-6.37	-.0009	1.85	1.0	-.28	-.6
17	-.5	.14	-.32	.91	.54	.64	.0037	-.043	-.0001	2.19	1.0	-.02	-.6
18	-.5	.14	-.91	.91	.54	.88	.0047	.28	.0015	3.0	1.0	.31	-.6

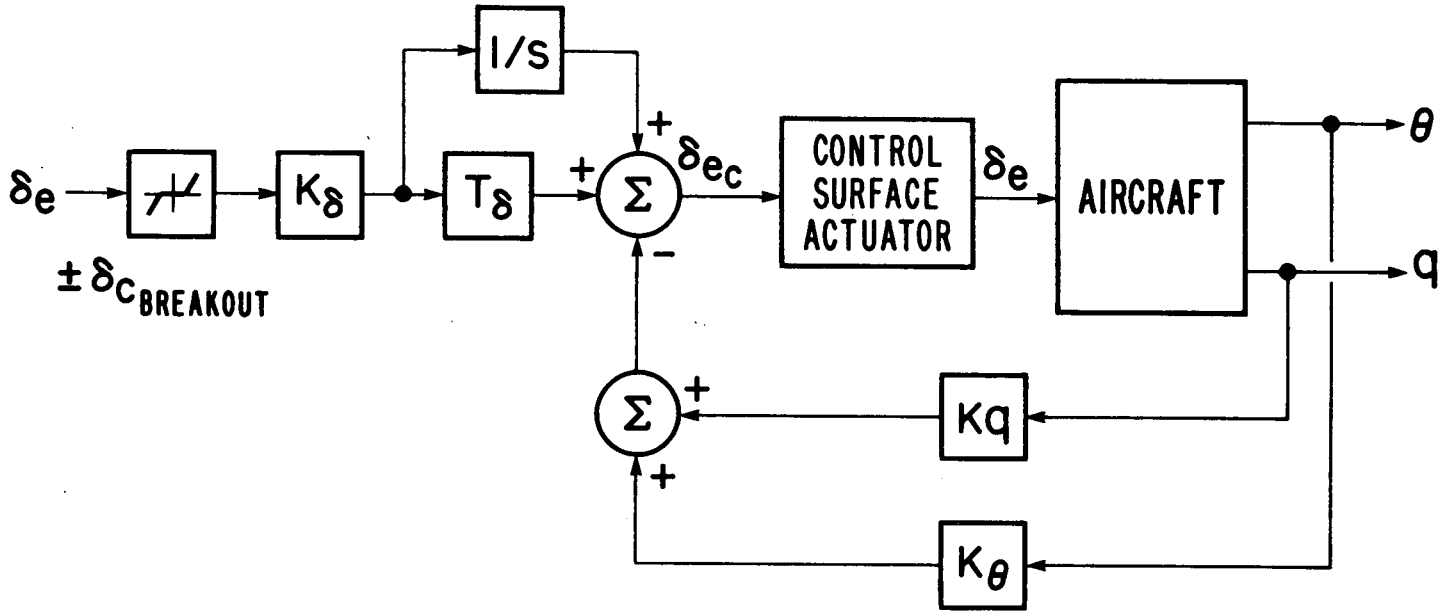

Figure 1. Block Diagram of Pitch Rate Command/Attitude Hold Control System

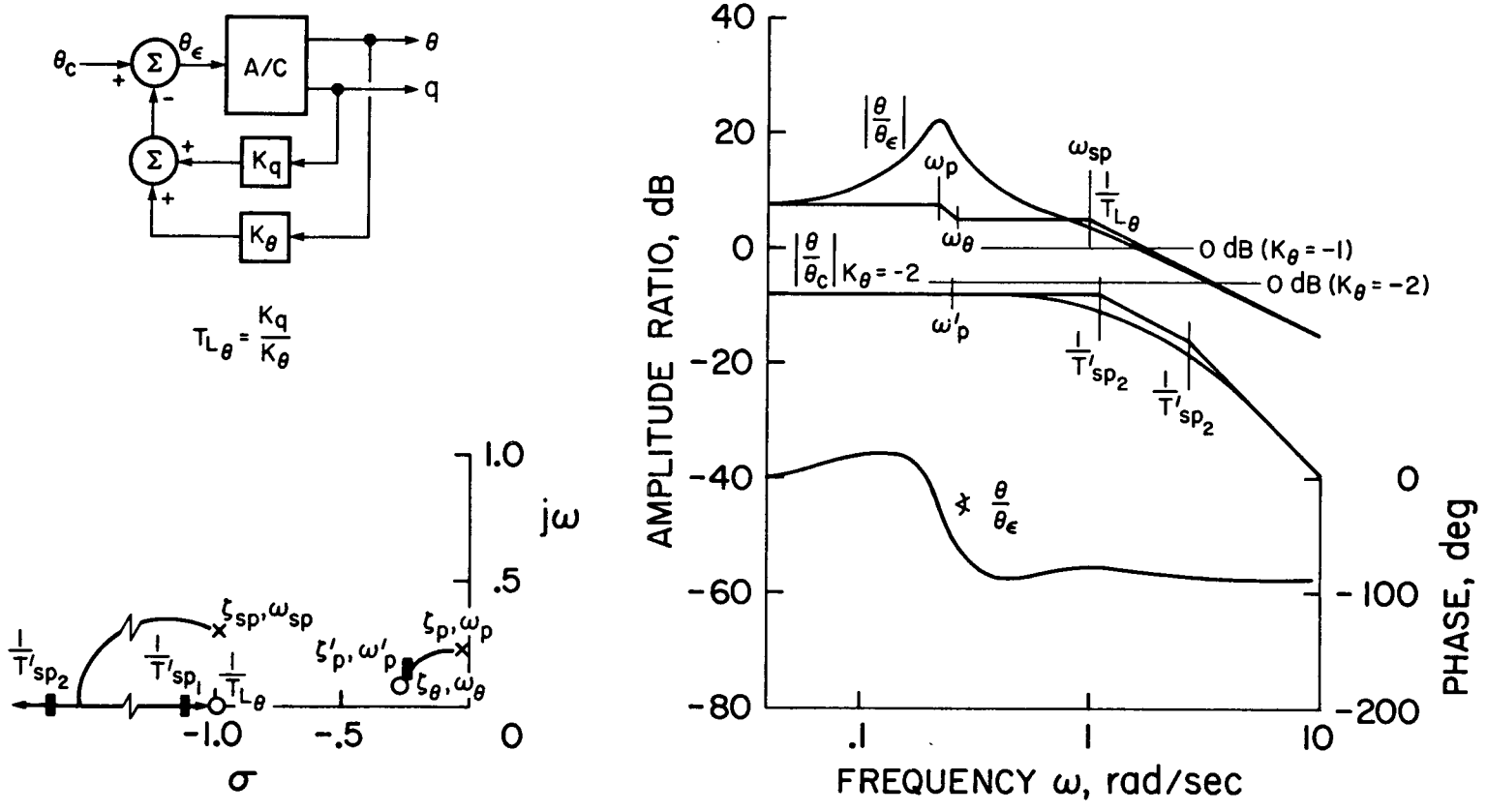

Figure 2. Effect of Pitch Rate and Attitude Stabilization on Pitch Attitude Control Characteristics

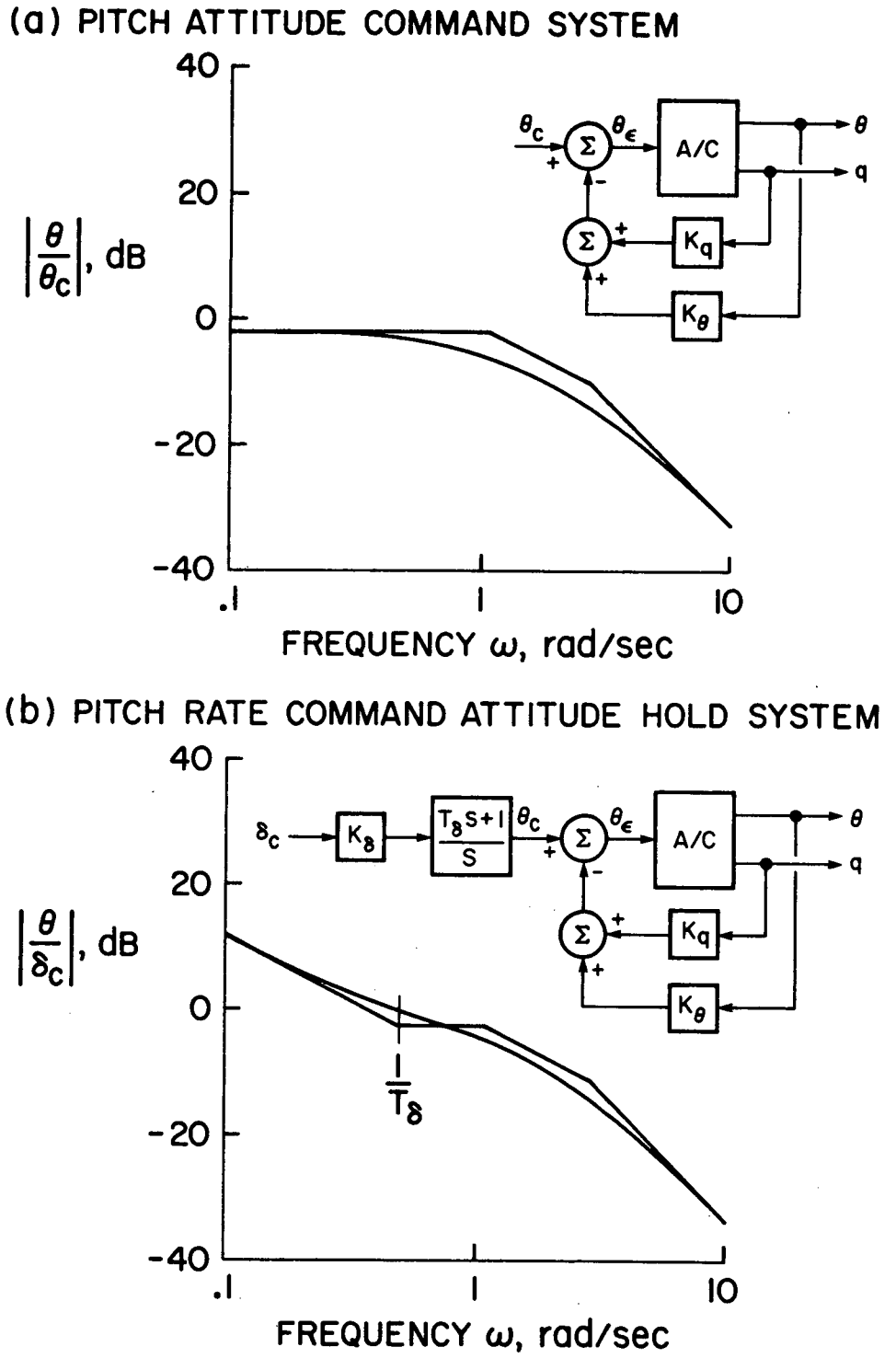

Figure 3. Comparison of Pitch Attitude and Rate Command System Transfer Functions

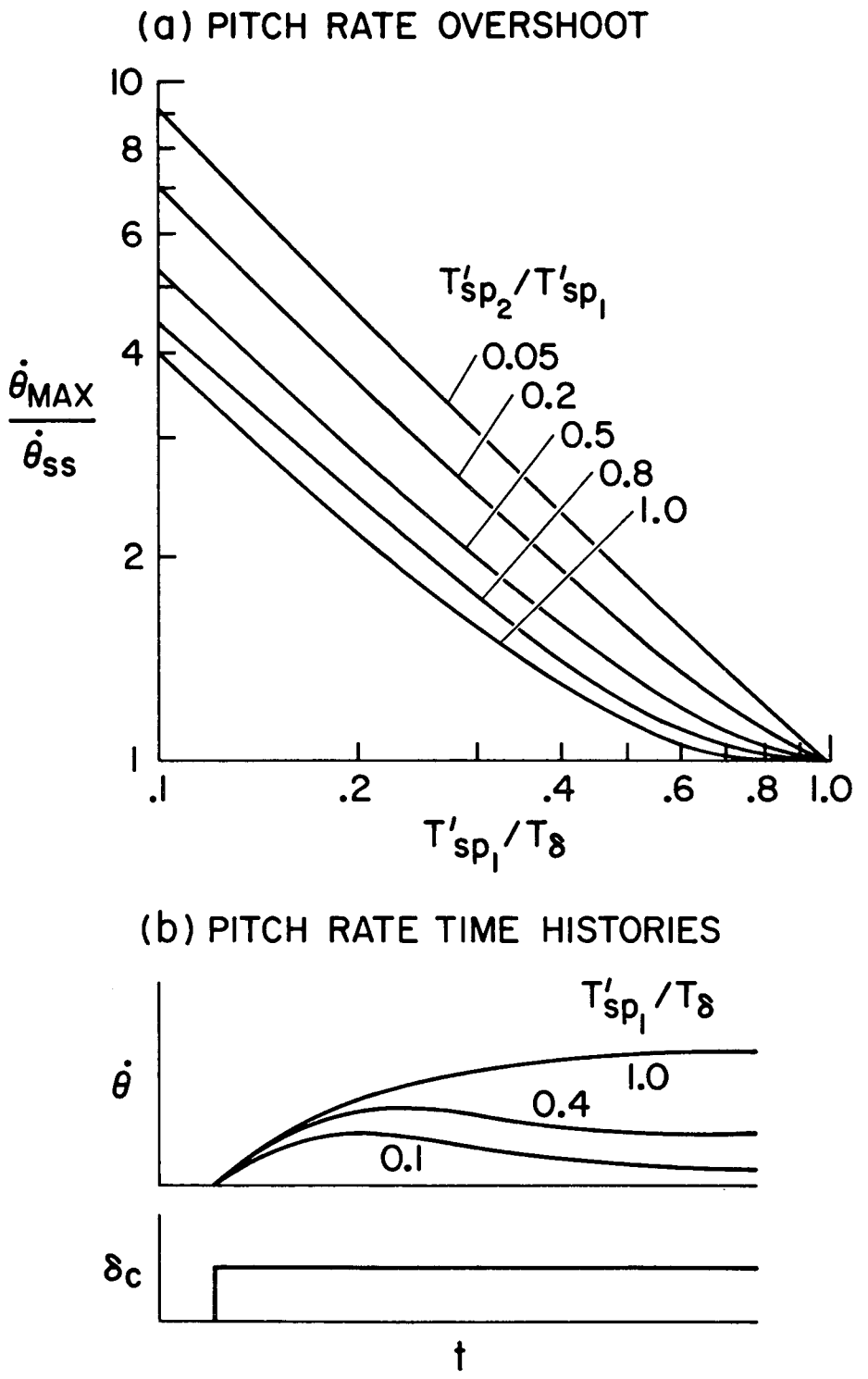

Figure 4. Pitch Rate Response Characteristics

- Block Diagram

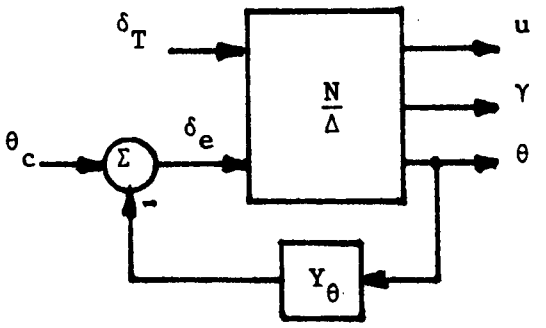

- Equations of Motion

$$\begin{bmatrix} \Delta \end{bmatrix} \begin{bmatrix} u \\ \alpha \\ \theta \\ \gamma \end{bmatrix} = \begin{bmatrix} X_{\delta_e} & X_{\delta_T} \\ Z_{\delta_e} & Z_{\delta_T} \\ M_{\delta_e} & M_{\delta_T} \\ 0 & 0 \end{bmatrix} \begin{bmatrix} \delta_e \\ \delta_T \end{bmatrix}$$

where:

$$\begin{bmatrix} \Delta \end{bmatrix} = \begin{bmatrix} s-X_u & -X_{\dot{\alpha}}s-X_\alpha & (V_o \sin\alpha_o - Xq)s + g\cos\theta_o & 0 \\ -Z_u & (V_o - Z_{\dot{\alpha}})s - Z_\alpha & -(V_o+Z_q)s + g\sin\theta_o & 0 \\ -M_u & -M_{\dot{\alpha}}s-M_\alpha & s(s-M_q) & 0 \\ -\frac{\sin\theta_o}{V_o} & \cos\theta_o & -\cos\theta_o - \sin\theta_o \cdot \sin\alpha_o & 1 \end{bmatrix}$$

$$Y_\theta = K_\theta (T_{L_\theta} s + 1)$$

Figure 5. Block Diagram and Longitudinal Perturbation Equations of Aircraft with Pitch Attitude Stabilization

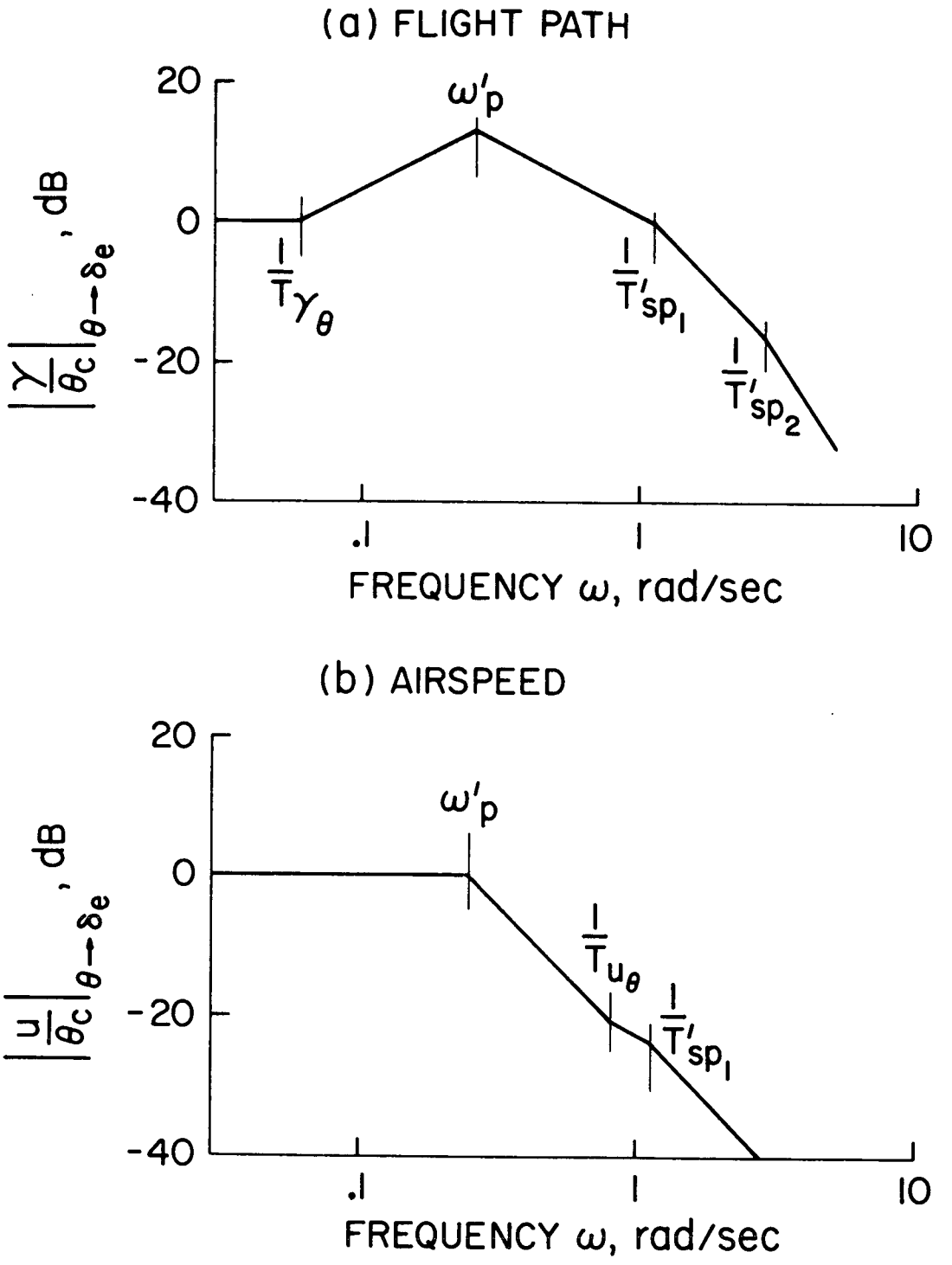

Figure 6. Examples of Transfer Functions for Flight Path and Airspeed Response to Attitude Command

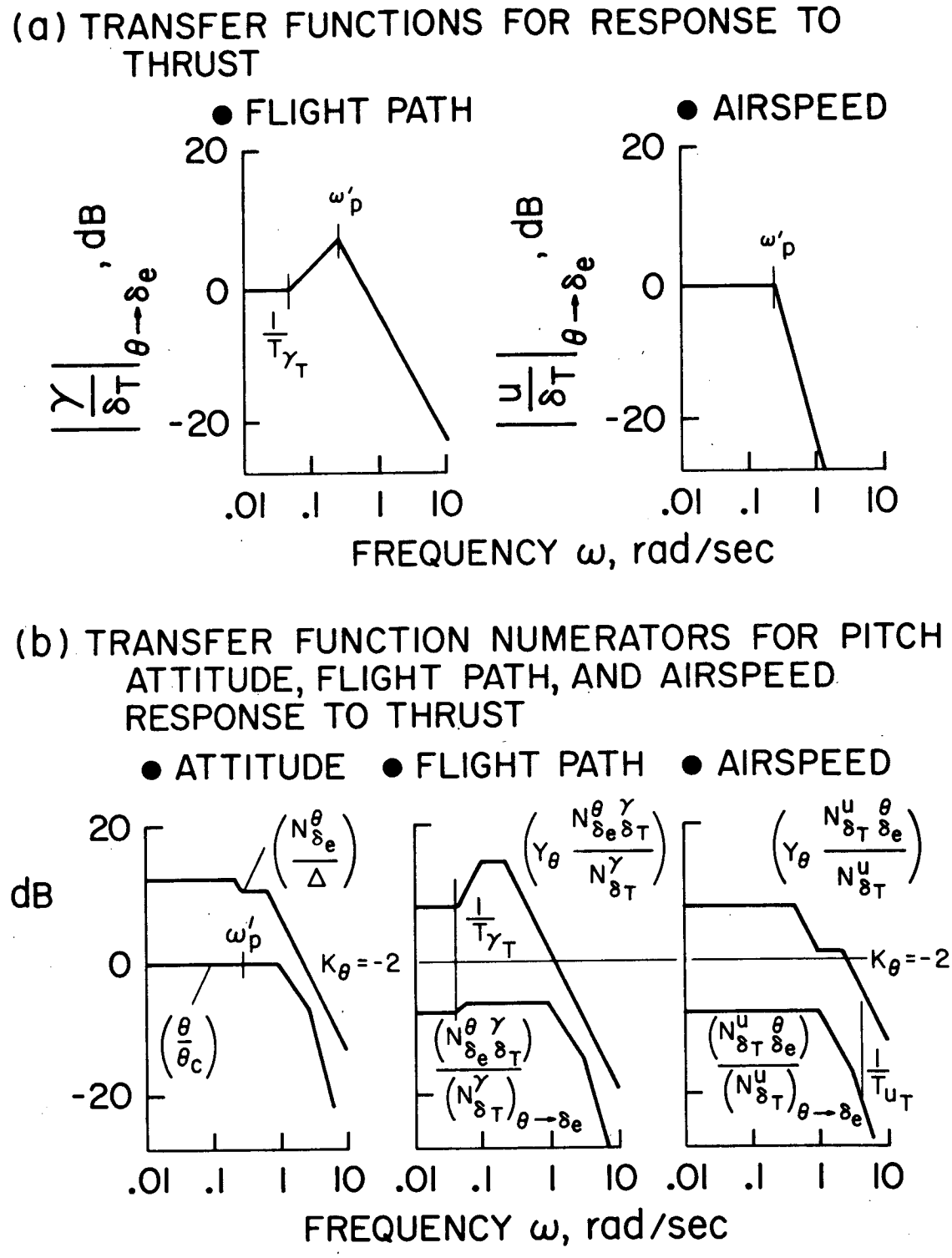

Figure 7. Examples of Transfer Functions for Flight Path and Airspeed Response to Thrust

$$\frac{R}{C} = A \frac{(S + 1/T)}{(S^2 + 2\zeta'_p \omega'_p S + \omega'^2_p)}$$

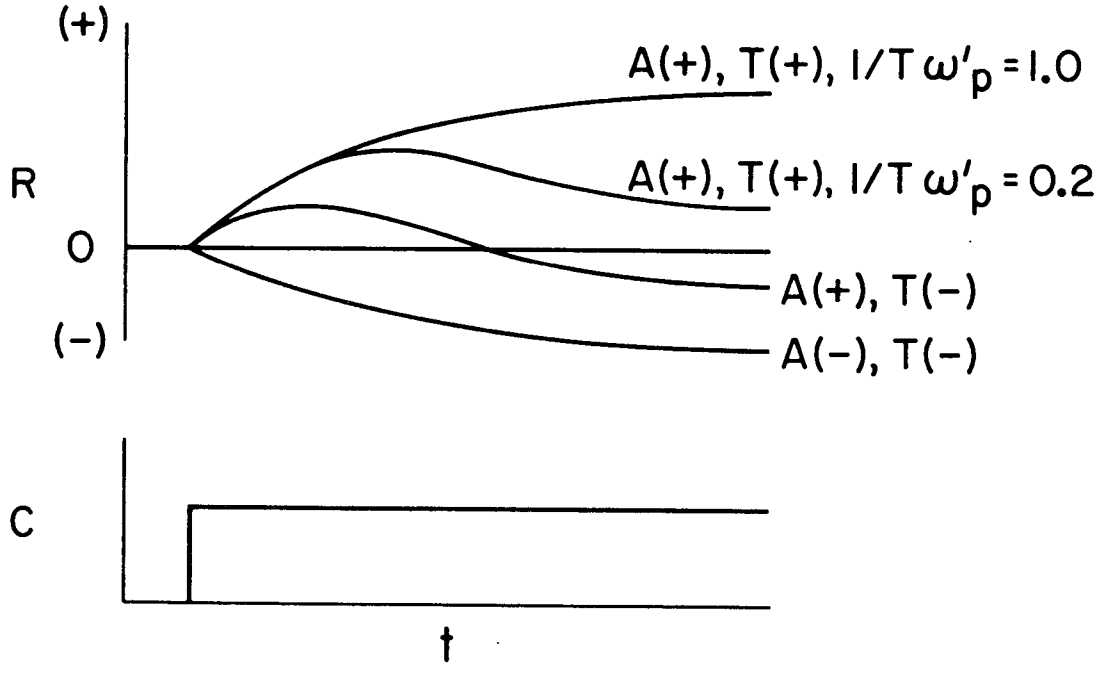

Figure 8. Examples of Time Response Characteristics

(a) FLIGHT PATH AND AIRSPEED RESPONSE TO CONTROLS

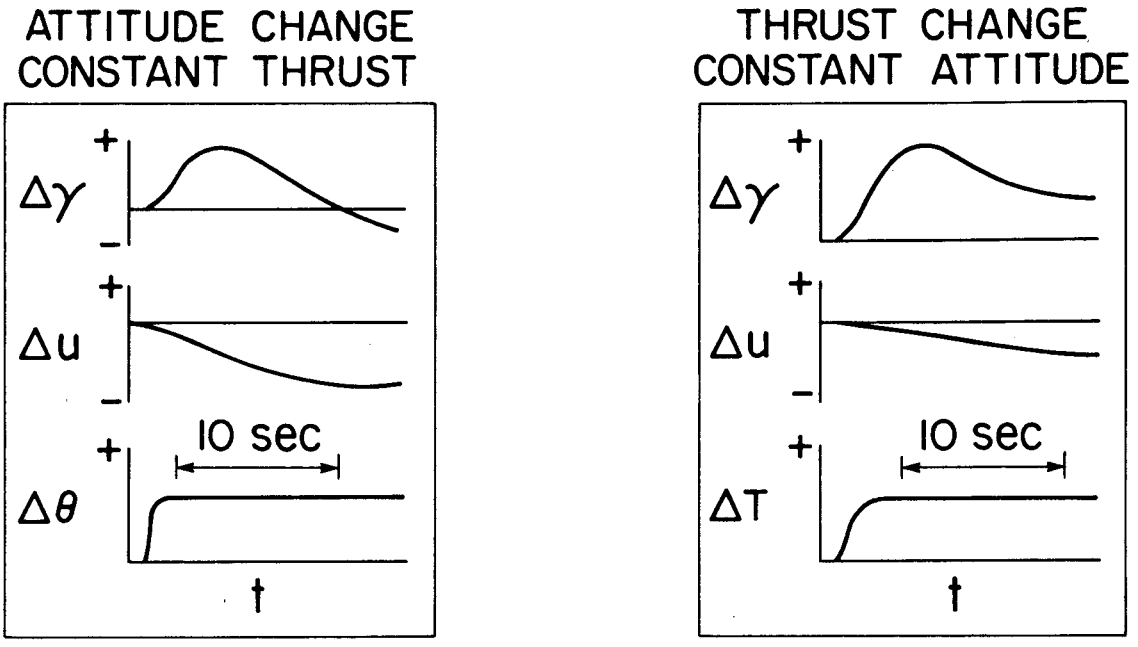

(b) CONTROL TECHNIQUE FOR INVESTIGATION

- STABILIZE PITCH ATTITUDE (PILOT OR SAS)
- SPEED CONTROL WITH ATTITUDE
- FLIGHT PATH CONTROL WITH THRUST

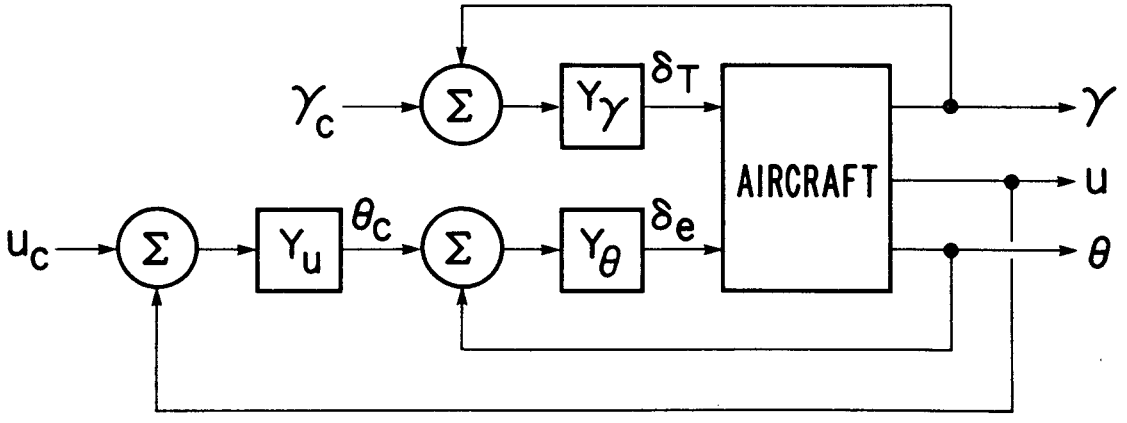

Figure 9. Control Technique

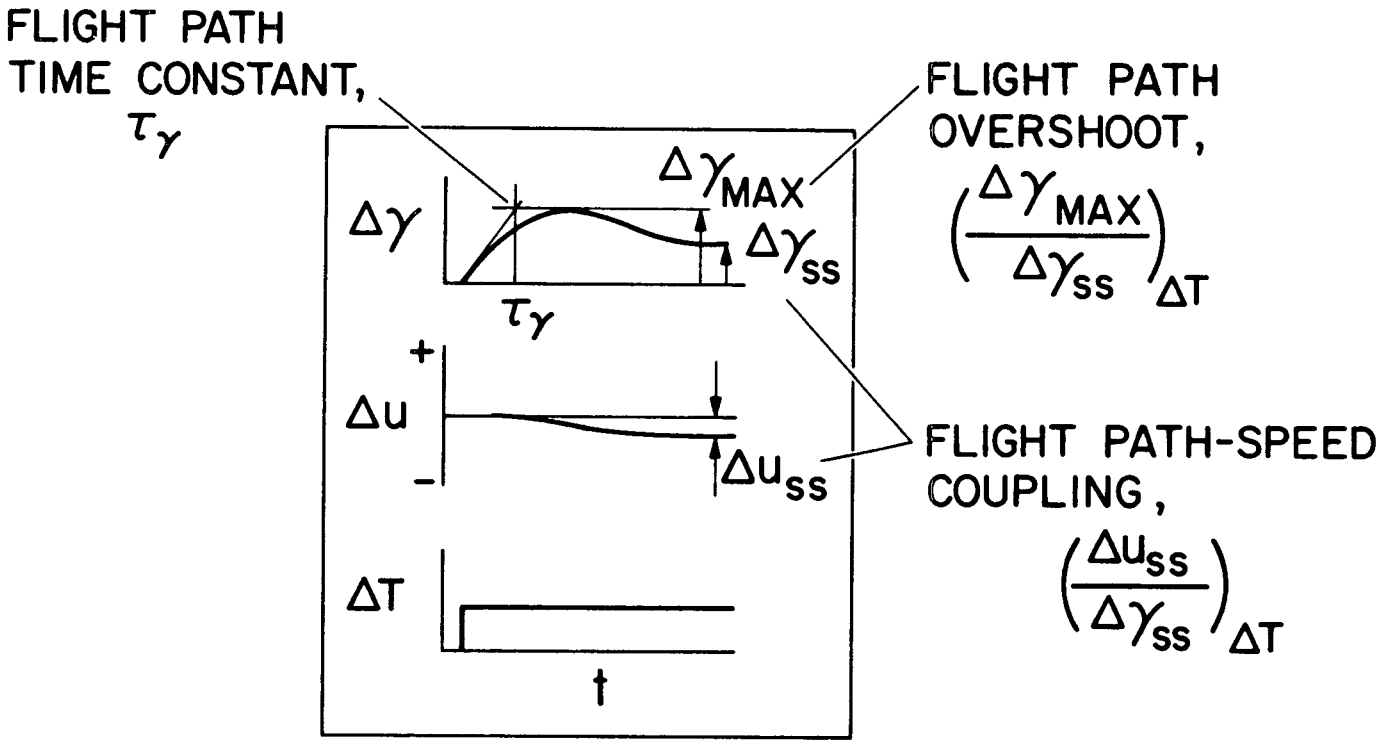

Figure 10. Characteristics of Response of Flight Path and Airspeed to Thrust

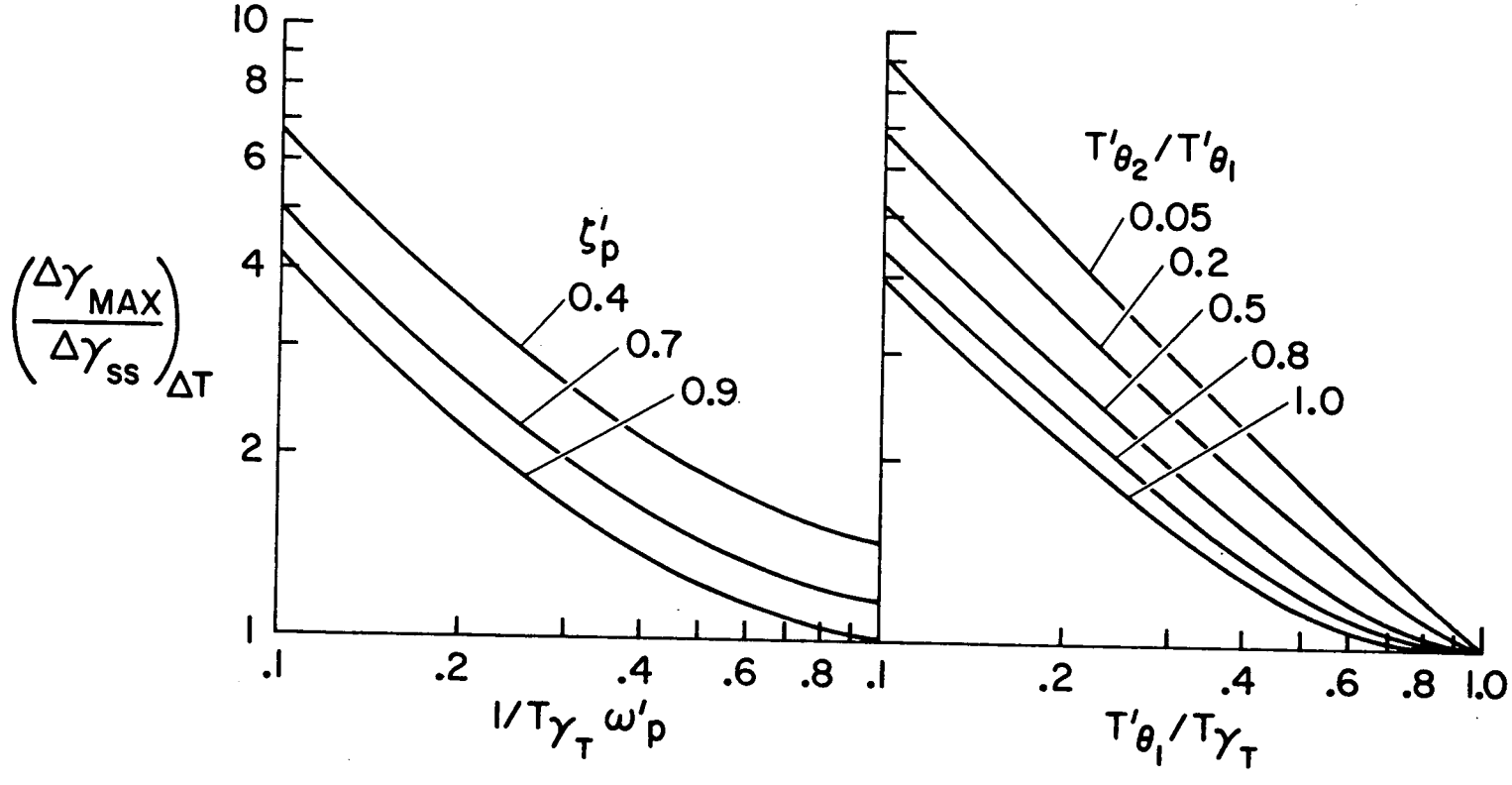

Figure 11. Contributions to Flight Path Overshoot Ratio

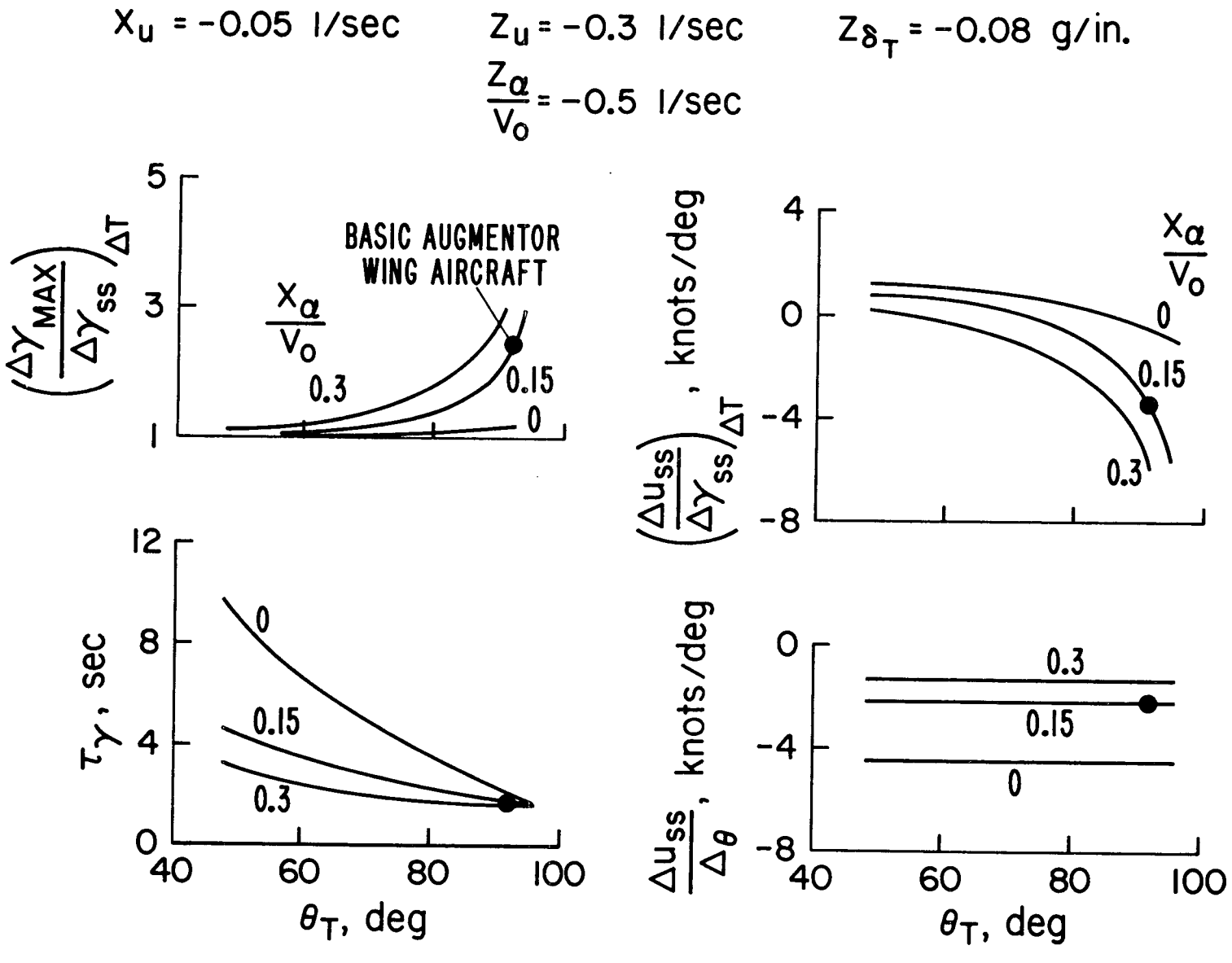

Figure 12. Contribution of Thrust Inclination and Drag due to Lift

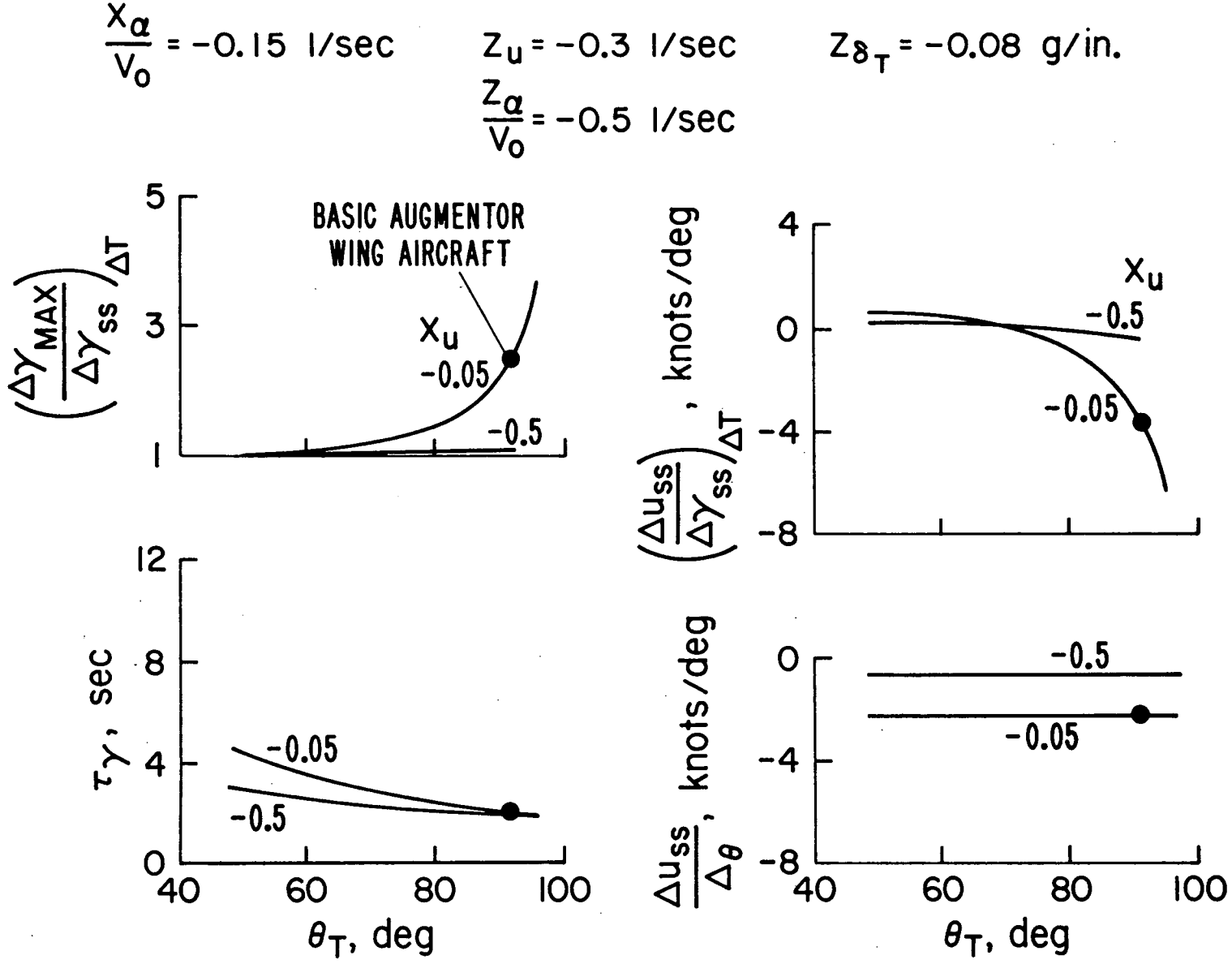

Figure 13. Contribution of Thrust Inclination and Axial Velocity Damping

$$\left(\frac{\Delta u_{ss}}{\Delta \gamma_{ss}}\right)_{\Delta T} = \frac{T\gamma_T \omega'^2_p}{Z_u/V_o}\left[1+\left(\frac{1}{T\gamma_T \omega'^2_p}\right)\frac{Z_\alpha}{V_o}\right]$$

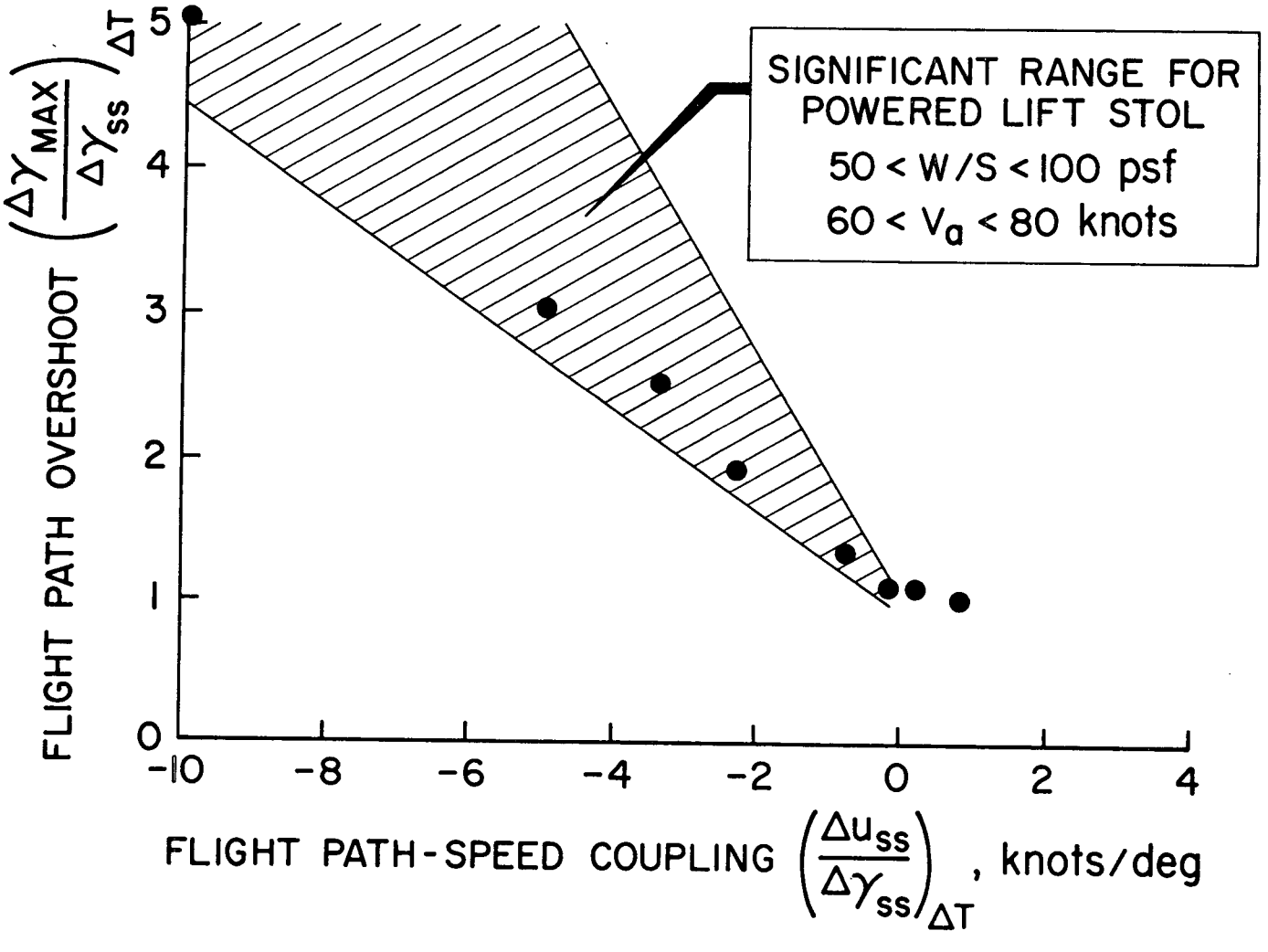

Figure 14. Interrelationship Between Flight Path Overshoot and Flight Path - Speed Coupling Parameters

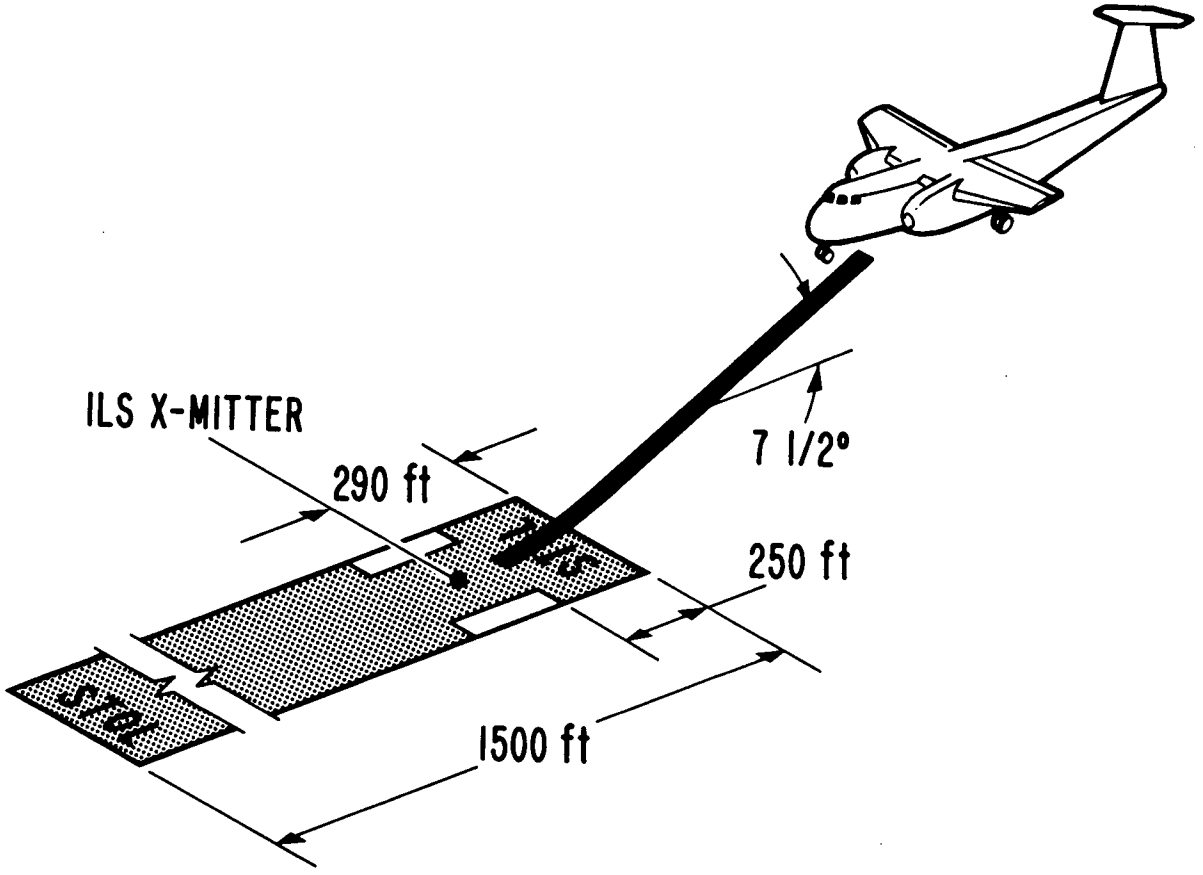

Figure 15. STOL Port Configuration

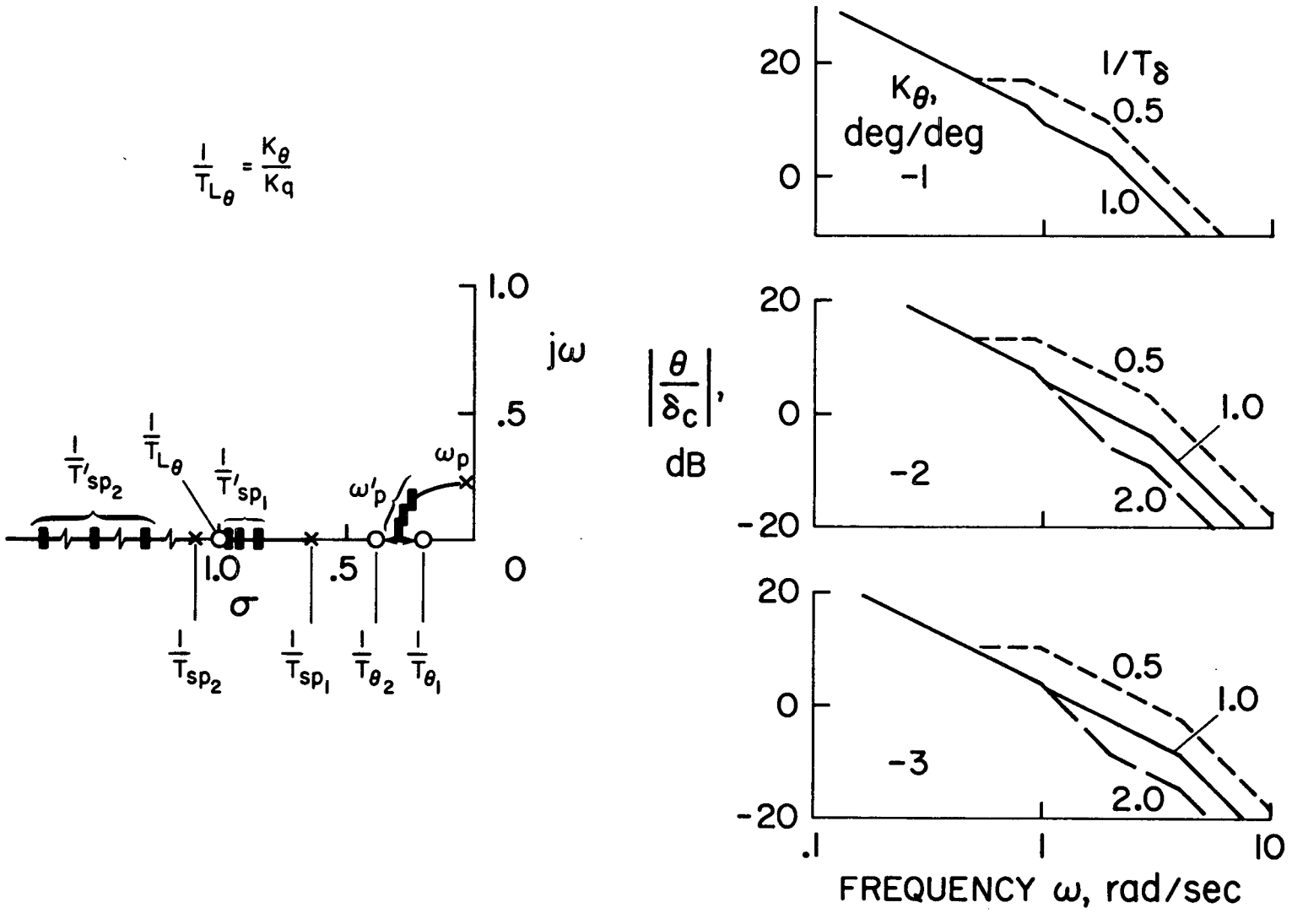

Figure 16. Closed Loop Roots and Transfer Functions for Pitch Rate Command Attitude Hold Configurations

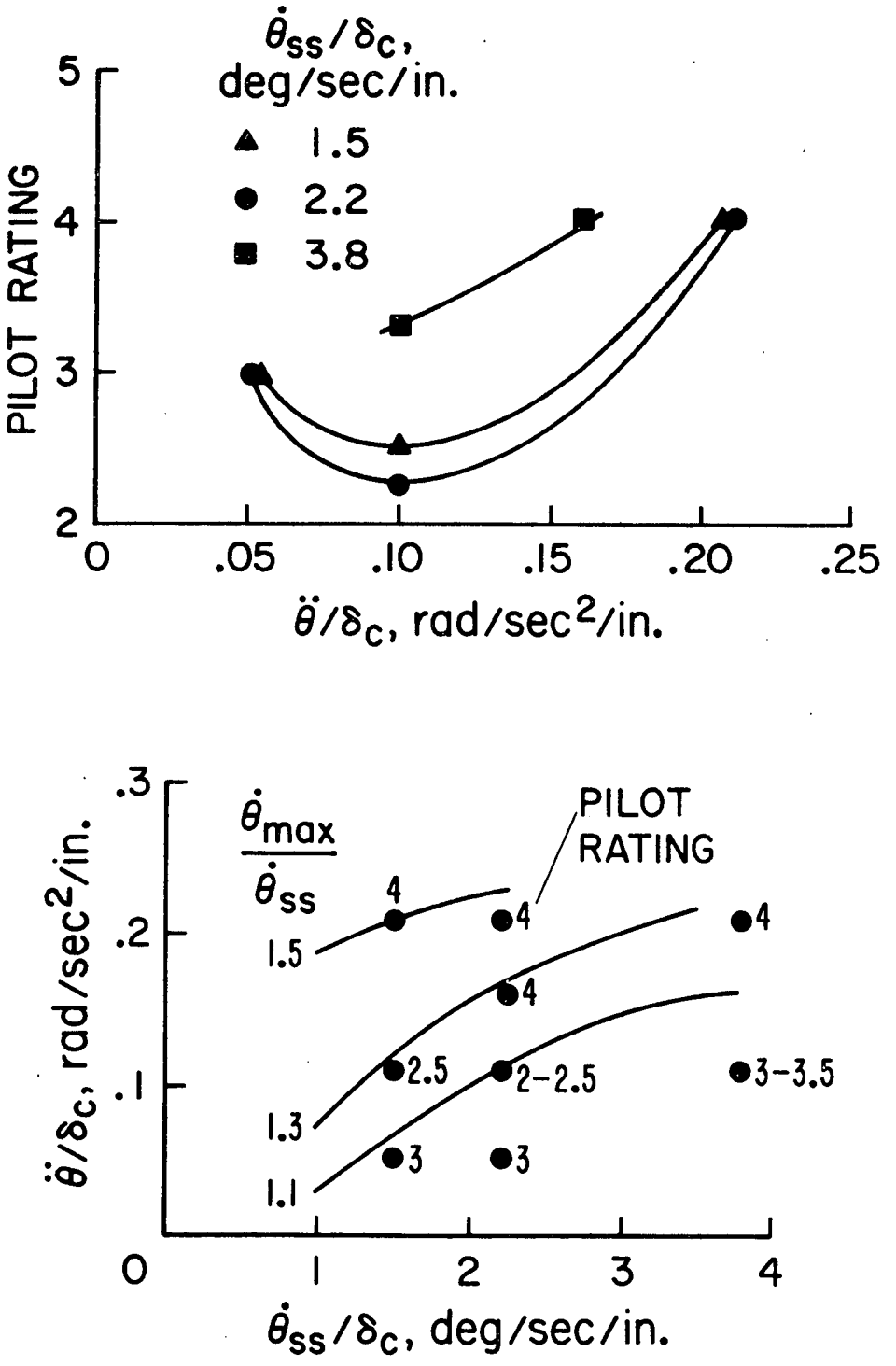

Figure 17. Pilot Ratings for Pitch Rate Command/Attitude Hold Systems

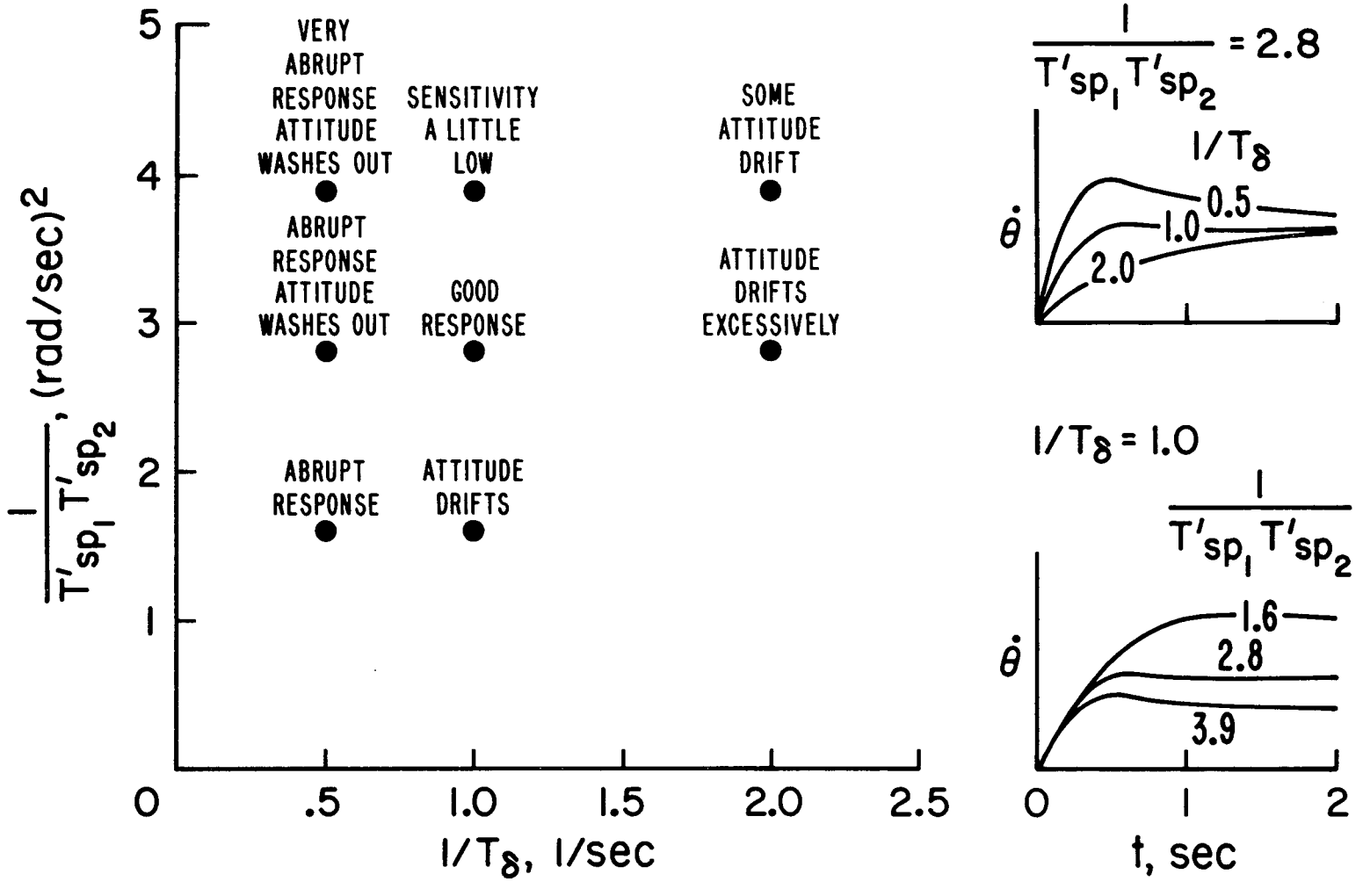

Figure 18. Pilot Commentary for Pitch Rate Command/Attitude Hold Systems

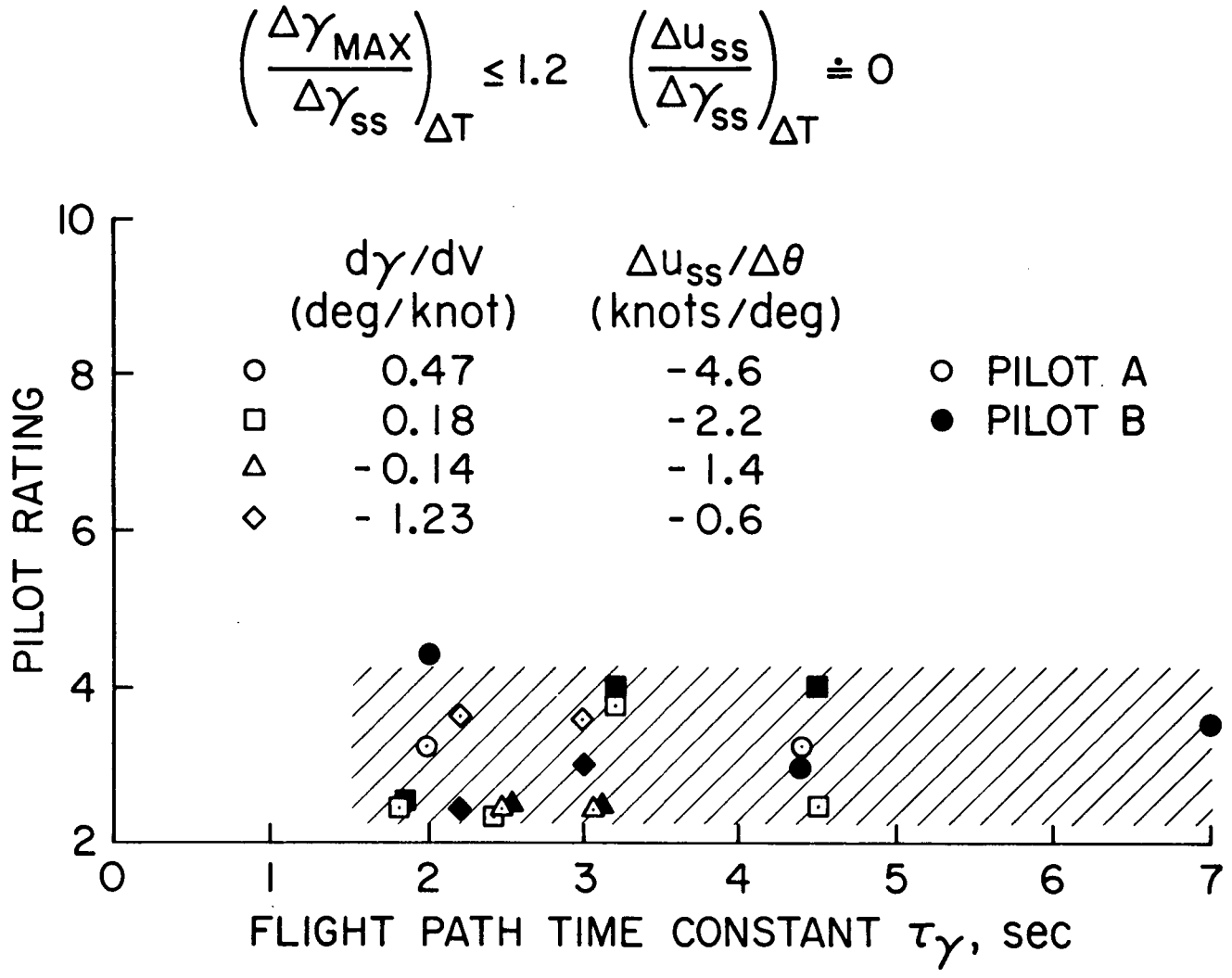

Figure 19. Influence of Initial Flight Path Response

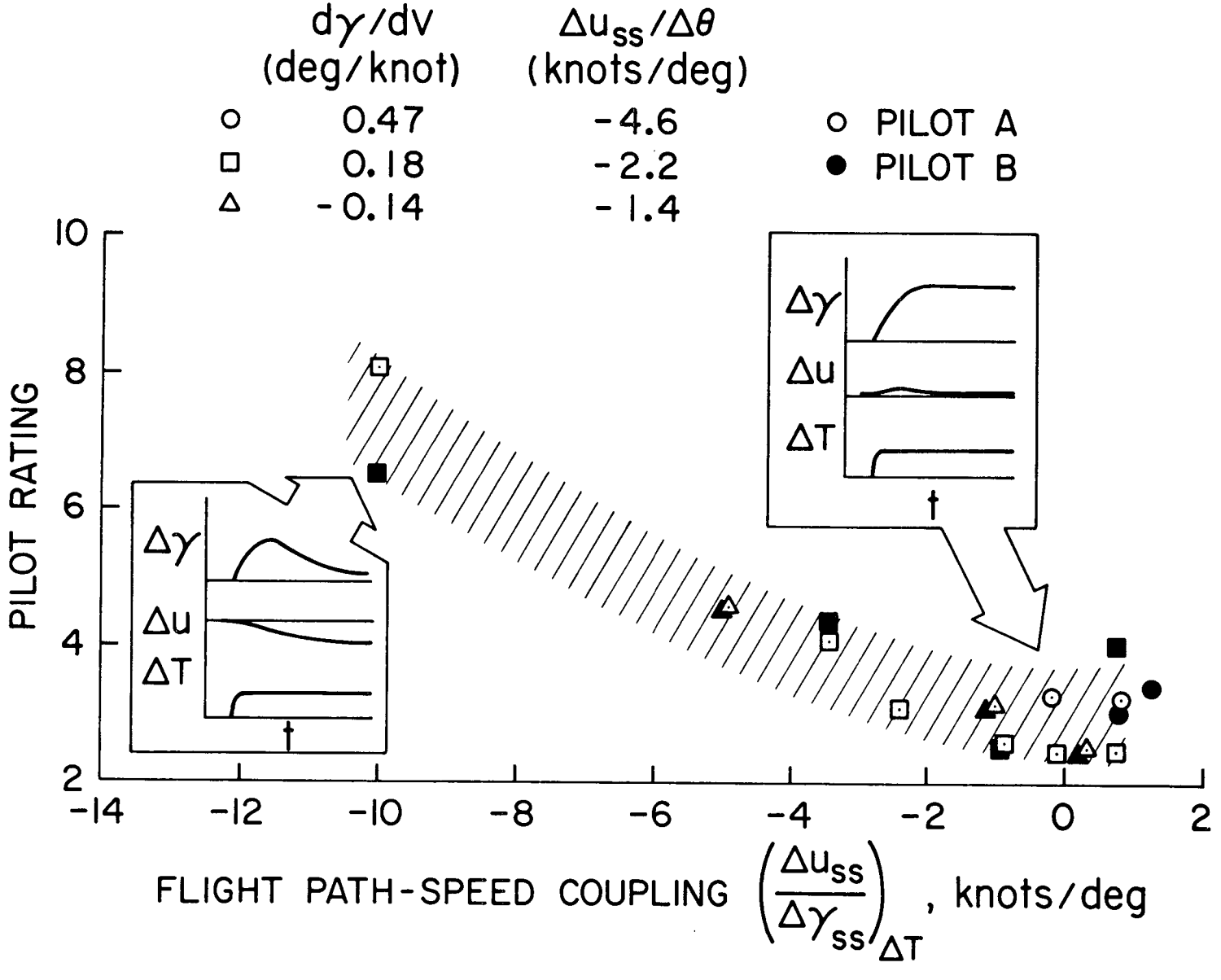

Figure 20. Influence of Flight Path - Airspeed Coupling

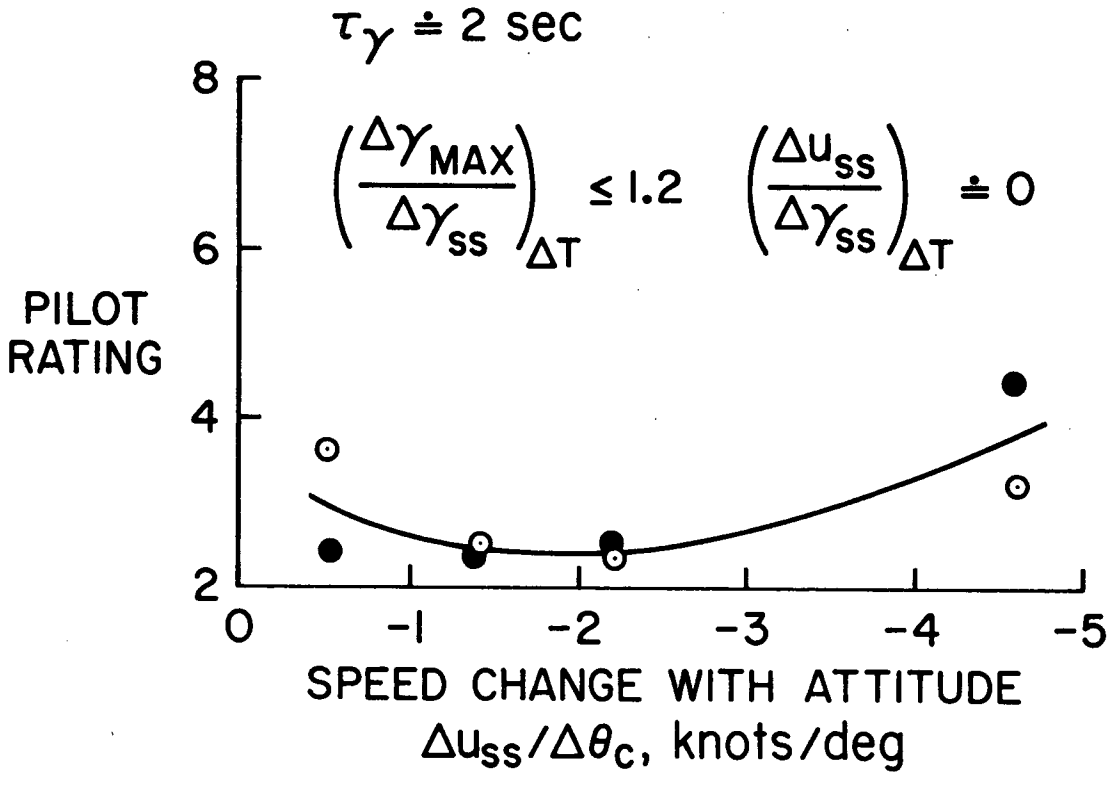

Figure 21. Speed Response to Pitch Attitude

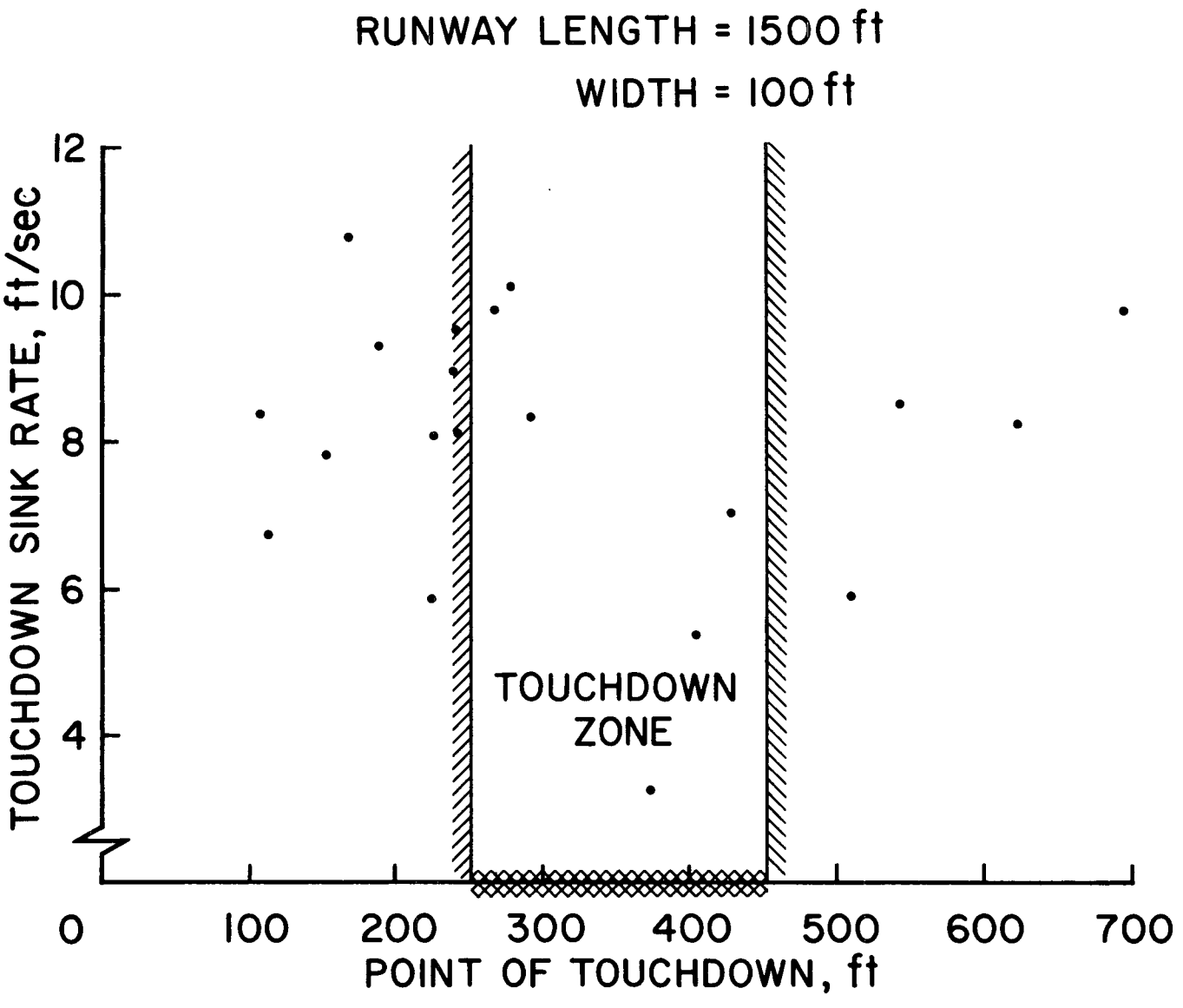

Figure 22. Landing Precision - All Test Configurations

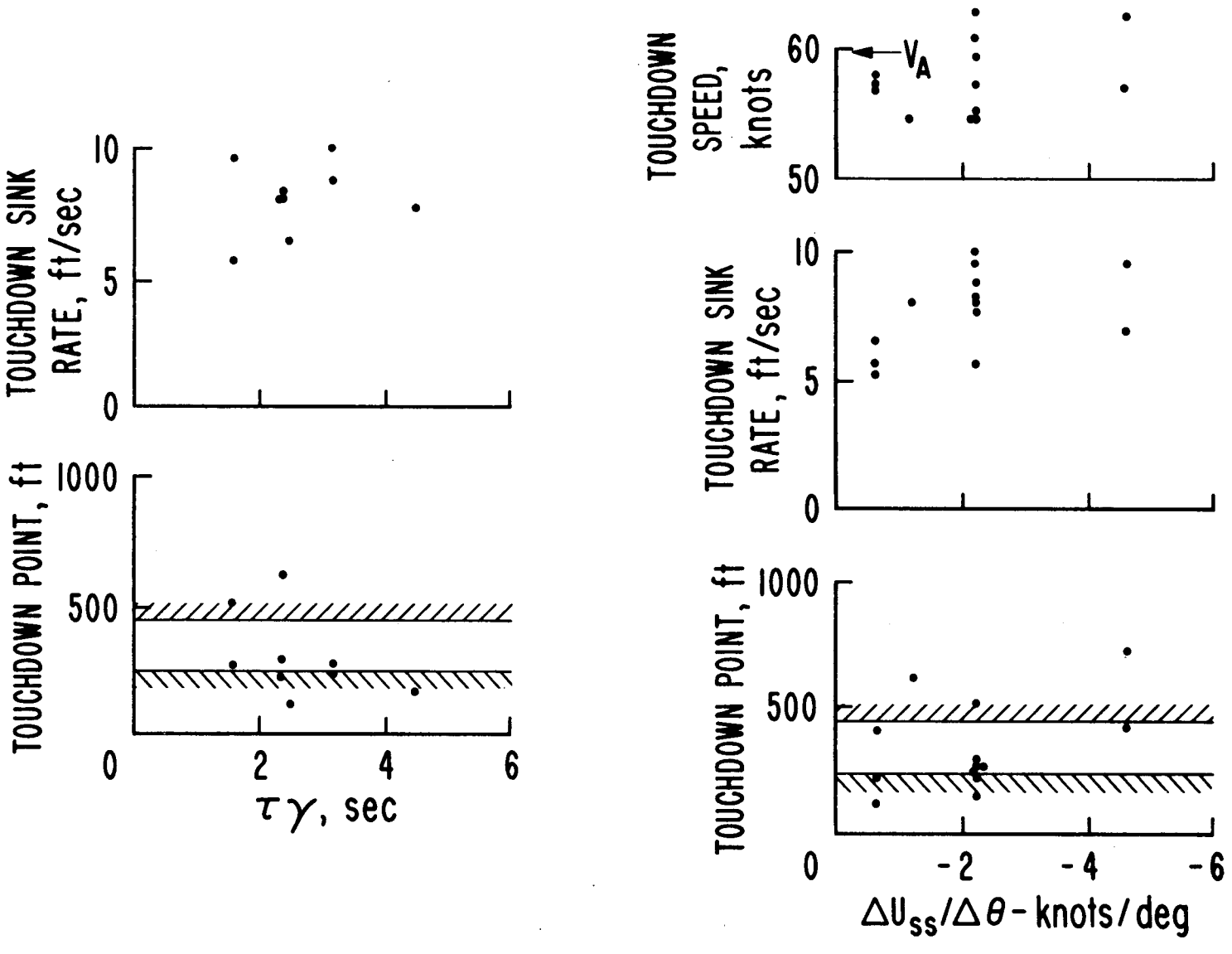

Figure 23. Effects of Flight Path Response to Thrust and Speed Response to Attitude on Landing Precision

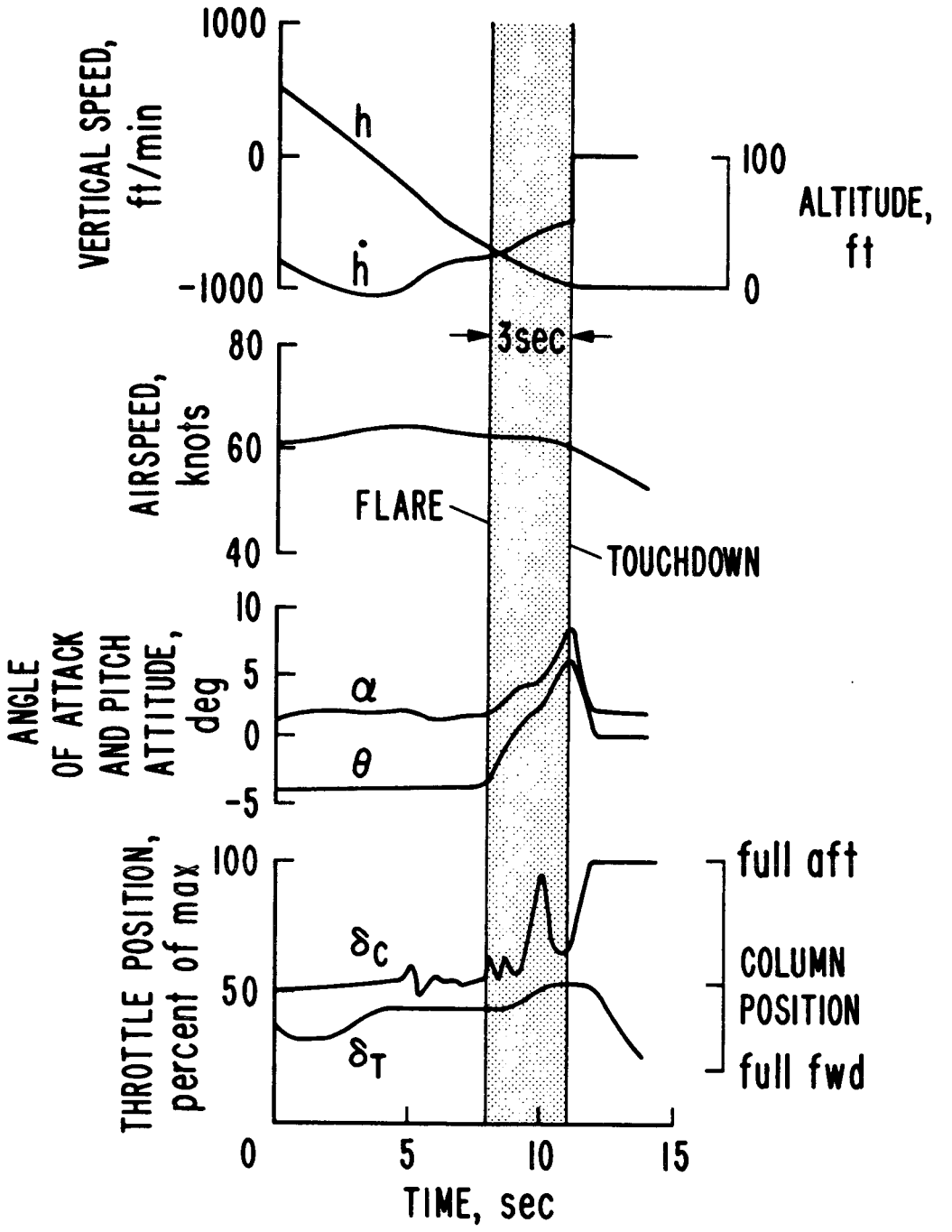

Figure 24. Example STOL Landing

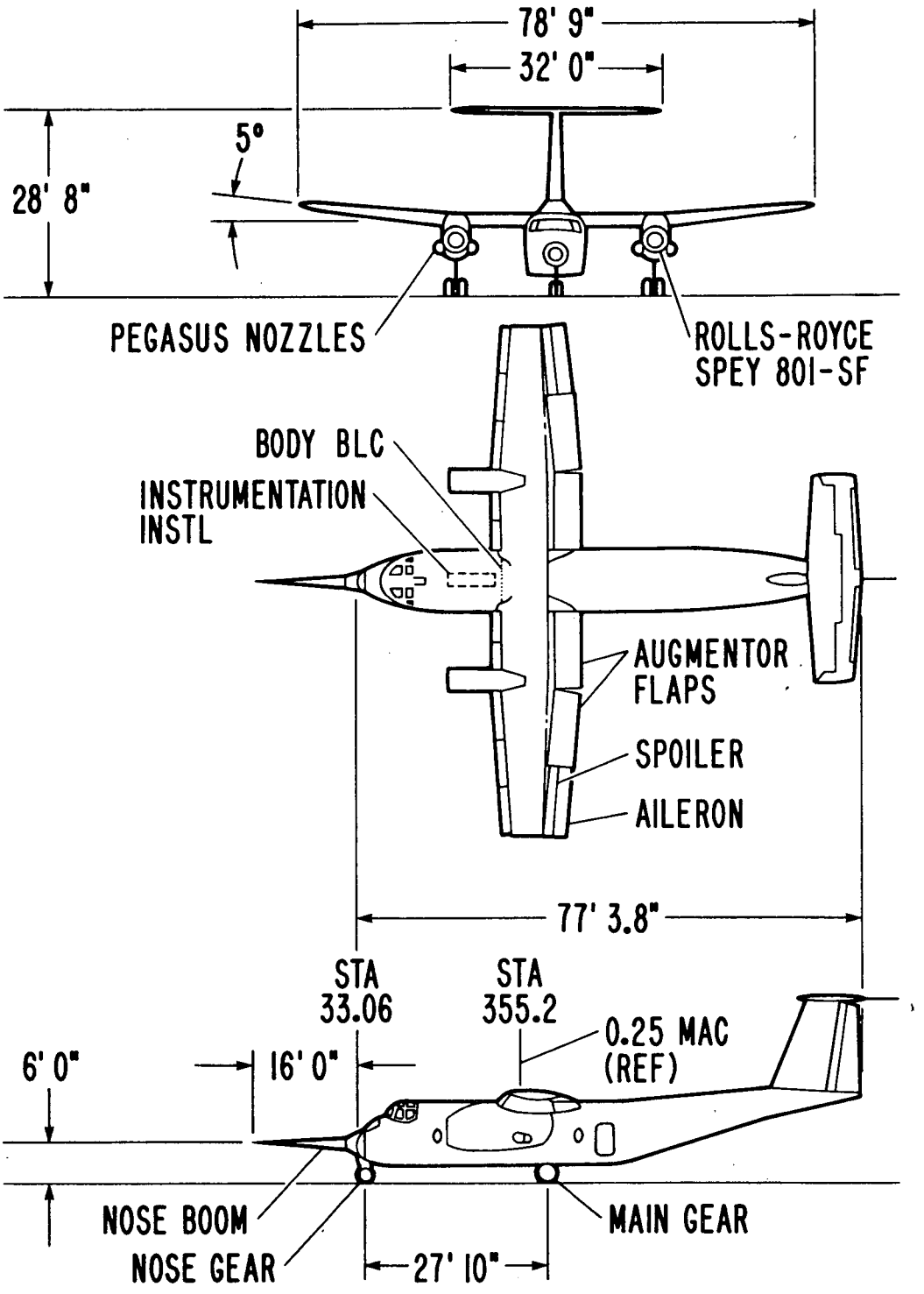

Figure A1. Augmentor Wing Jet STOL Research Aircraft

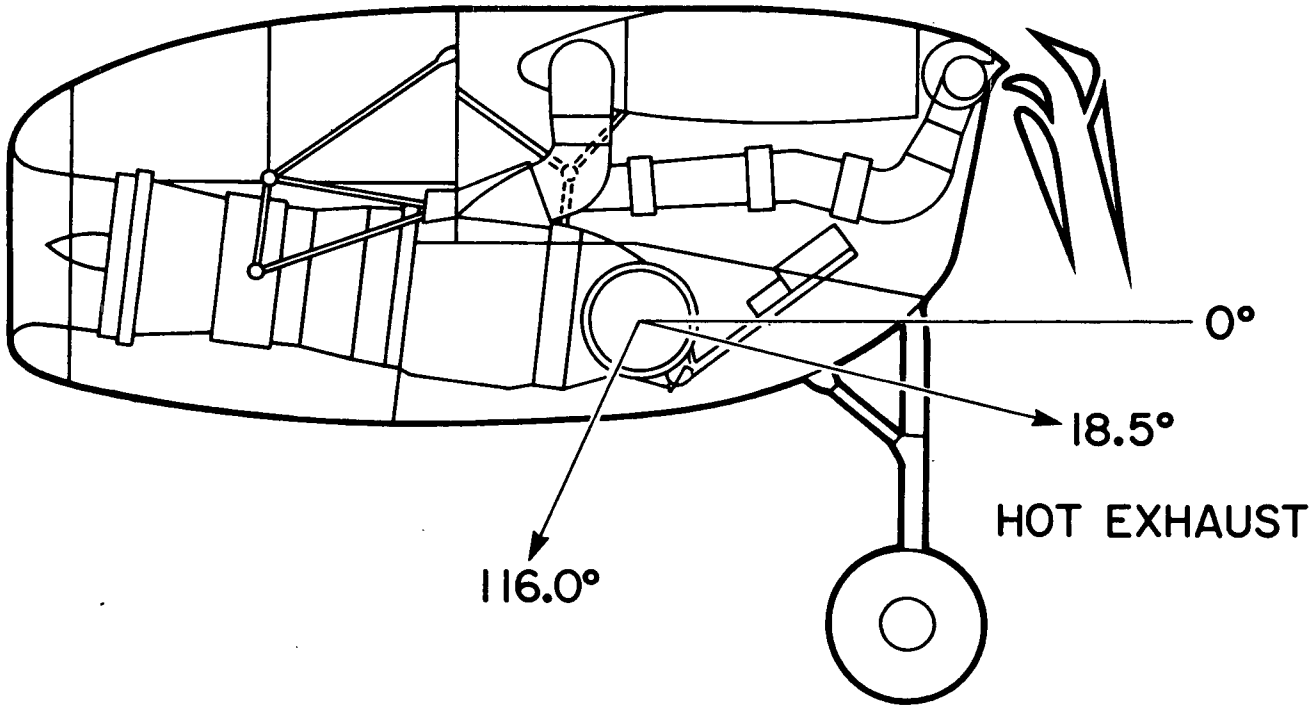

Figure A2. Rolls Royce Spey 801 SF Engine
and Pegasus Nozzle Arrangement

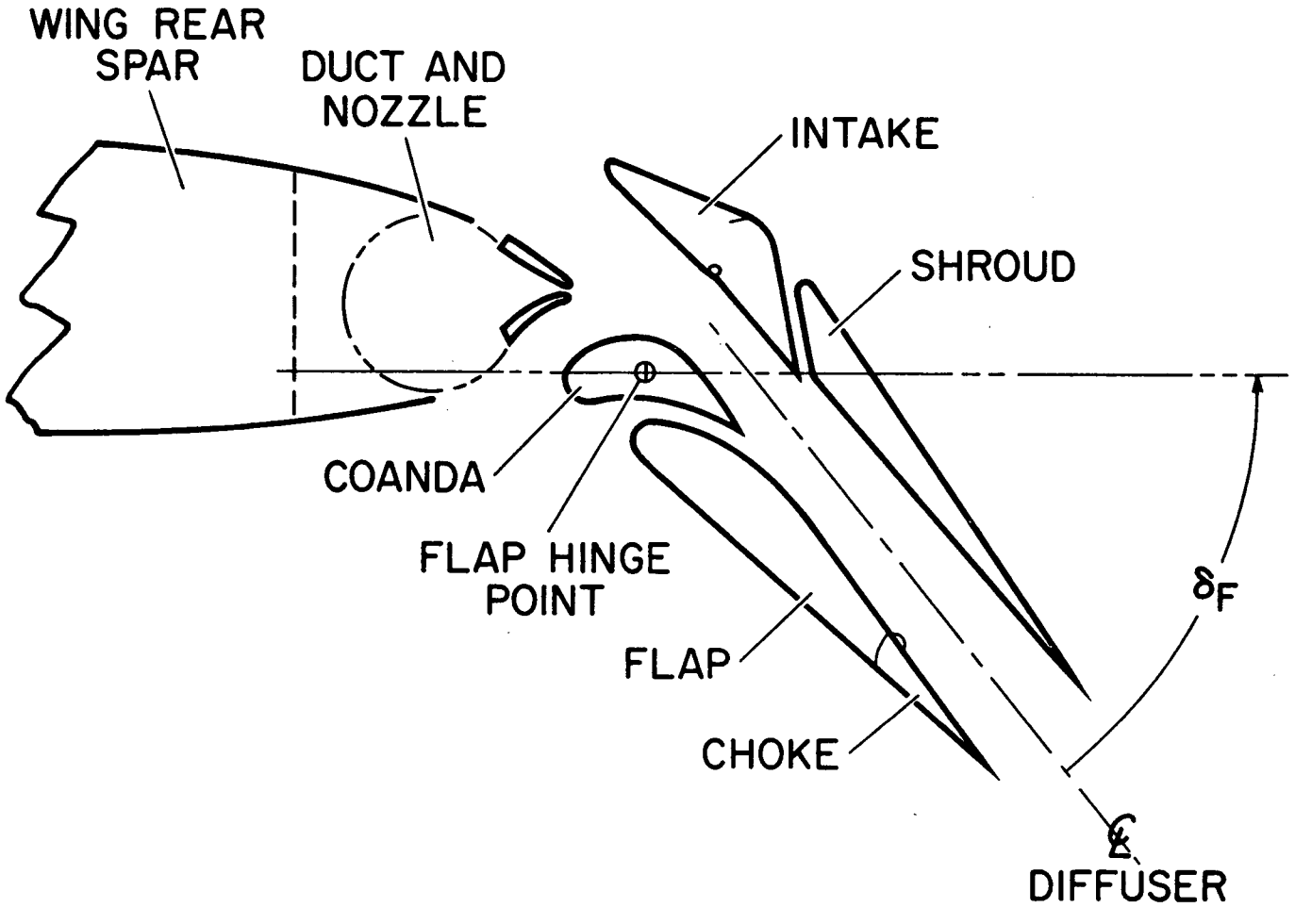

Figure A3. Augmentor Flap

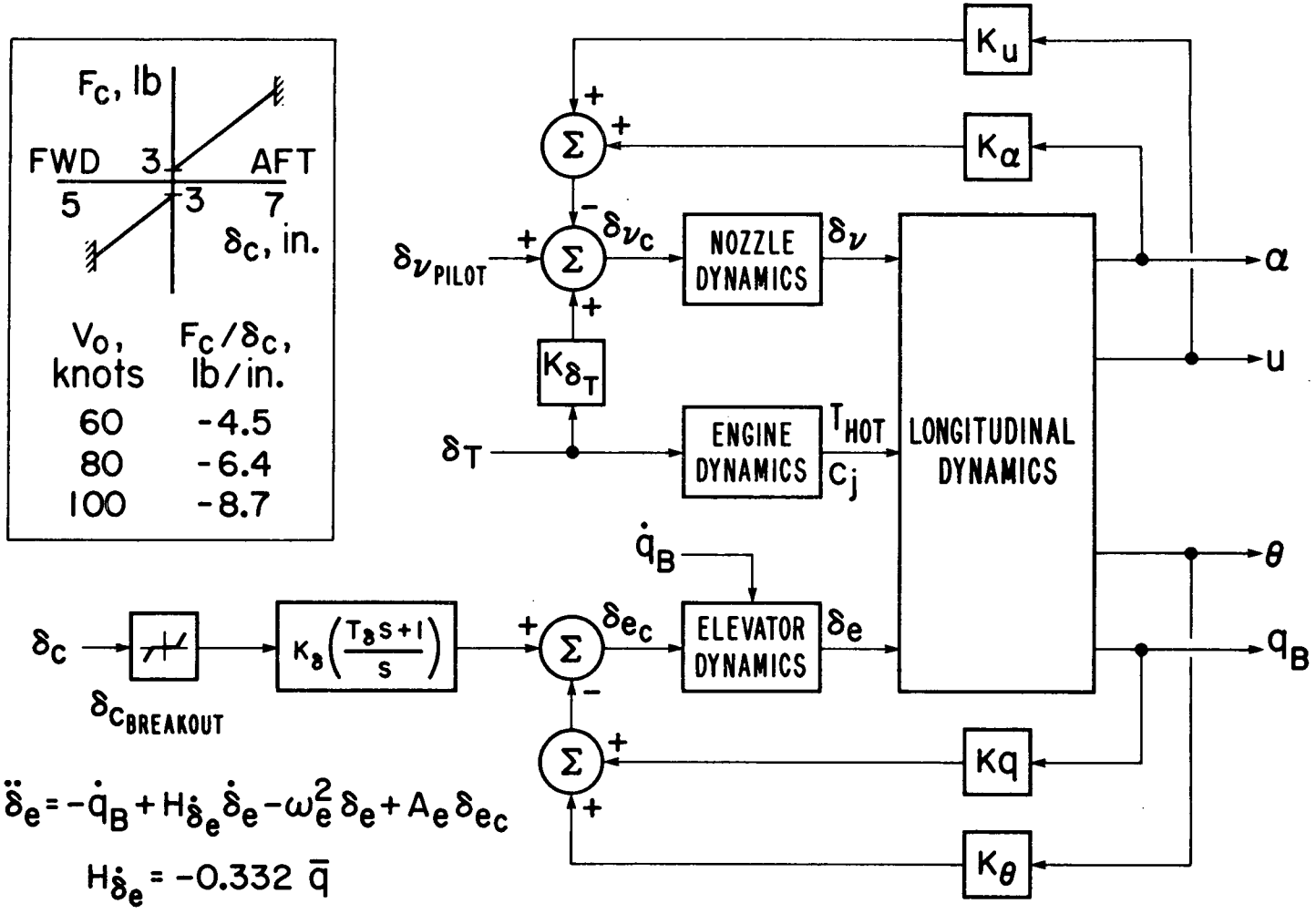

$$\ddot{\delta}_e = -\dot{q}_B + H_{\dot{\delta}_e}\dot{\delta}_e - \omega_e^2\,\delta_e + A_e\,\delta_{e_c}$$

$$H_{\dot{\delta}_e} = -0.332\ \bar{q}$$

$$\omega_e^2 = 2.04\ \bar{q} + A_e$$

$$A_e = \frac{13.35 + 17.44\ \bar{q}}{1 + 0.108\ \bar{q}}$$

Figure A4. Longitudinal Control System

AUGMENTOR WING AIRCRAFT LONGITUDINAL DYNAMICS

Landing Approach Condition

Flight-Loading Conditions

V_o = 60 knots	GW = 40,000 lbs
γ = -7.5 deg	I_x = 300,000 slug-ft^2
α = 2.74 deg	I_y = 207,000 slug-ft^2
δ_f = 65 deg	I_z = 500,000 slug-ft^2
δ_ν = 90 deg	I_{xz} = 36,000 slug-ft^2
T_{HOT} = 6380 lbs	X_{cg} = 29.2% mac

Stability Derivatives (Body Axis)		Response Characteristics	
X_u	= -.052 1/sec	ζ_p	= .15
X_α	= 14 ft/sec^2/rad	ω_p	= .22 rad/sec
$X_{\dot{\alpha}}$	= .11 ft/sec	$1/T_{sp_1}$	= .62 rad/sec
X_q	= .25 ft/sec	$1/T_{sp_2}$	= 1.2 rad/sec
X_{δ_e}	= -.34 ft/sec^2/rad		
X_{δ_ν}	= -4.85 ft/sec^2/rad	$1/T_{\theta_1}$	= .18 rad/sec
X_{δ_T}	= -.000036 ft/sec^2/lb	$1/T_{\theta_2}$	= .37 rad/sec
Z_u	= -.29 1/sec	$1/T_{u_\theta}$	= .84 rad/sec
Z_α	= -52. ft/sec^2/rad	$1/T_{\gamma_\theta}$	= -.06 rad/sec
$Z_{\dot{\alpha}}$	= -1.56 ft/sec		
Z_q	= -3.44 ft/sec	$1/T_{u_T}$	= 5.94 rad/sec
$Z_{\delta e}$	= -4.9 ft/sec^2/rad	$1/T_{\gamma_T}$	= .049 rad/sec
$Z_{\delta\nu}$	= 0.		
Z_{δ_T}	= -.00168 ft/sec^2/lb	F_c/a_z	= 57.2 lbs/g
		$\ddot{\theta} / \delta_c$	= .07 rad/sec^2/inch

M_u = .00051 rad/ft sec

M_α = -.3 rad/sec^2/rad

$M_{\dot{\alpha}}$ = -.42 1/sec

M_q = -.93 1/sec

M_{δ_e} = -1.2 rad/sec^2/rad

M_{δ_ν} = -.074 rad/sec^2/rad

M_{δ_T} = .000002 rad/sec^2/lb

τ_γ = 1.56 sec

$(\Delta\gamma_{max}/\Delta\gamma_{ss})\Delta T$ = 2.4

$(\Delta u_{ss}/\Delta\gamma_{ss})\Delta T$ = -3.45 kts/deg

$\Delta u_{ss}/\Delta\theta$ = -2.2 kts/deg